The bacteria-protist link as a main route of dissolved organic matter across contrasting productivity areas ~~in~~ on the Patagonian Shelf

M. Celeste López-Abbate[1], John E. Garzón-Cardona[1,2], Ricardo Silva[3], Juan-Carlos Molinero[4], Laura A. Ruiz-Etcheverry[5,6,7], Ana M. Martínez[8], Azul S. Gilabert[1,9], Rubén J. Lara[1]

[1] Instituto Argentino de Oceanografía (CONICET-UNS), Camino La Carrindanga km 7.5, 8000 Bahía Blanca, Argentina.

[2] Departamento de Química, Universidad Nacional del Sur. ~~Departamento de Química~~, 8000 Bahía Blanca, Argentina.

[3] Instituto Nacional de Investigación y Desarrollo Pesquero (INIDEP), ~~Paseo Victoria Ocampo Nº1 (~~B7602HSA~~)~~, Mar del Plata, Buenos Aires, Argentina.

[4] Institut de Recherche pour le Développement (IRD), UMR248 MARBEC, IRD/CNRS/IFREMER/UM, Sète Cedex, France.

[5] Departamento de Ciencias de La Atmósfera y Los Océanos, Facultad de Ciencias Exactas y Naturales, Universidad de Buenos Aires (DCAO, FCEN-UBA), ~~Intendente Guiraldes 2160,~~ Ciudad Universitaria, Pabellón II 2do. Piso, C1428EGA Ciudad Autónoma de Buenos Aires, Argentina

[6] Centro de Investigaciones Del Mar y La Atm~~ó~~sfera (CIMA/CONICET-UBA), C1428EGA Ciudad Autónoma de Buenos Aires, Argentina

[7] Instituto Franco-Argentino para El Estudio Del Clima y Sus Impactos (IRL-IFAECI/CNRS-CONICET-UBA), C1428EGA Ciudad Autónoma de Buenos Aires, Argentina

[8] Instituto de Química del Sur (INQUISUR-CONICET), Universidad Nacional del Sur, 8000 Bahía Blanca, Argentina.

[9] Departamento de Geografía y Turismo (DGyT), Universidad Nacional del Sur, 8000 Bahía Blanca, Argentina.

Correspondence to: Celeste López-Abbate (mclabbate@iado-conicet.gob.ar)

Abstract

While the sources of dissolved organic matter (DOM) in the open ocean are relatively well identified, its fate due to microbial activity is still evolving. Here, we explored how microbial community structure, growth, and grazing of phytoplankton and heterotrophic bacteria influenced the DOM pool and the transformation of its fluorescent fraction ~~(FDOM). D during d~~ilution experiments were performed during the productive season~~in~~ on the Patagonian Shelf (SW Atlantic Ocean), a region of intense biological activity, with peak productivity observed at the shelf break front. ~~This area constitutes a global hotspot of carbon sequestration due to intense biological productivity which peaks at the shelf break front. The productive stations at the shelf break front featured a food web primarily based on phytoplankton and heterotrophic bacteria, while less productive mid-shelf stations showed greater dependence of protistan predators on bacterial biomass.~~ Although phytoplankton biomass was higher than that of bacteria, protists selectively preyed on the latter, which exhibited faster growth rates, denoting ~~high~~ trophic specificity of grazers. High trophic efficiency was suggested by the biomass distribution of protistan consumers and their prey, which predominantly exhibited a top-heavy pyramid structure. An exception to this pattern was observed at the highly productive shelf break front, where a traditional bottom-heavy pyramid emerged, indicating that most phytoplankton evaded protist predation despite evidence of herbivory~~Trophic efficiency and omnivory favored a bottom-heavy biomass distribution, characterized by consumer biomass dominance over producers, except in highly productive stations influenced by nutrient-rich upwelling waters, where a typical pyramid structure was observed~~. Bacterial consumption of DOM appeared uncoupled from its total amount but was influenced by DOM complexity, while the bacterial production of humic-like substances from protistan plankton precursors observed in most experiments highlighted a potential pathway for carbon sequestration. Protistan grazers also significantly influenced DOM dynamics by scaling their DOM contribution in response to the intensity of grazing on heterotrophic bacteria, regardless of productivity levels. This effect likely arises from~~Our results showed that in addition to the commonly accepted factors such as phytoplankton growth stage and bacterial community composition, DOM accumulation versus consumption is also linked to bacterial grazing. Intense grazing on heterotrophic bacteria promoted DOM accumulation, likely by~~ reducing the number of active, DOM-consuming bacteria and by providing egestion DOM compounds ~~to the DOM pool. Moreover, bacterial consumption of DOM appeared uncoupled from its total amount but was influenced by FDOM properties~~. These findings suggest that under high bacterial growth rate that follows the onset of the productive season, protistan grazers act as a link between bacterial biomass and higher trophic levels. However, as bacterial grazing intensifies, they can simultaneously facilitate the accumulation of a fraction of DOM.~~, partially diverting DOM lysate production by virus.~~

1. Introduction

Marine microbes have consensual impact on human life due to their climate-active role that stems from their ecosystem functions and broad predominance in marine biomass (Cavicchioli et al., 2019). The balance between microbial climate roles, i.e., CO_2 fixation, nutrient regeneration, and carbon sequestration, has consequential buffering effects on the currently unbalanced global carbon cycle (Hutchins and Fu, 2017). The prediction of microbial climate roles, however, requires a deep understanding of microbial interactions since most metabolic outcomes are shaped by both resource supply and mortality sources. Protistan grazers along with viral lysis constitute the main sources of mortality of phytoplankton and prokaryotes in the ocean (Brussaard, 2004; Calbet and Landry, 2004; Weinbauer and Peduzzi, 1995). Both mortality sources create divergent carbon routes as viral lysis directs host biomass toward the dissolved organic matter (DOM) cycle and grazing may repackage bacterial and phytoplankton biomass inaccessible to mesozooplankton and fish larvae thus linking the microbial loop with higher trophic levels (Azam et al., 1983). Protistan grazers further impact element cycle by recycling nutrients, thus prolonging bloom formation (Sherr and Sherr, 2016), and by providing DOM from excretion and egestion (Kujawinski et al., 2004). The consequences of selective grazing upon prokaryotes or phytoplankton, however, are less well understood as it may result from the interplay of various factors. For example, while size-specific grazing prompt compositional shifts in phytoplankton (e.g., Kanayama et al., 2020), the more generalist grazing on bacteria implies that community composition tends to remain more stable under grazing pressure (Baltar et al., 2016). On the other hand, grazing on bacteria seems to remain close to bacterial production, specially under oligotrophic conditions (Sanders et al., 1992), but phytoplankton may temporally scape protistan grazing under favourable growth conditions thus allowing for bloom formation (Irigoien et al., 2005). The trophic transfer efficiency varies between phytoplankton and bacteria based food webs, with the former typically involving fewer carbon steps before reaching microcrustaceans (Berglund et al., 2007).

DOM represents the ocean's second most significant carbon reservoir after dissolved inorganic carbon, and its characteristics undergo alterations due to physical and biological processes on a daily basis (Spencer et al., 2007). The optical properties of DOM offer insights into its biochemical characteristics. The chromophoric fraction indirectly estimates phytoplankton DOM production (Romera Castillo et al., 2010), while fluorescence serves as an indicator of its biological and photochemical reactivity (Stedmon et al., 2003). While phytoplankton is the primary source of DOM in the ocean, other processes such as viral lysis and grazing also significantly influence its magnitude and complexity. The impact of protistan grazing on carbon pools, is driven by the remineralization of organic carbon and by the formation of DOM by reworking phytoplankton and bacterial biomass (Baña et al., 2014; Lund Paulsen et al., 2019; Nagata and Kirchman, 1992). However, the impact of selective grazing pressure on DOM-transforming prey, i.e., bacteria and phytoplankton, is less well understood.

Shelf areas represent global hotspots of carbon transformation not only due to their high productivity but also because of the intense interaction with terrestrial habitats and the local and meso-scale mixing processes connecting the euphotic zone with bottom sediments (Laruelle et al., 2018). The Patagonian Shelf is one of the largest continental shelf areas in the world and its more conspicuous feature is the presence of a 2500 km long upwelling front at the shelf break area characterized by recurrent spring blooms and intense geochemical transformation (Romero et al., 2006). Biological carbon fixation in this frontal area contributes substantially to

~~the sequestration of large amounts of carbon and constitutes one of the major CO_2 sinks at the global level (Kahl et al., 2017). The Patagonian Shelf, characterized by highly productive frontal regions, is particularly notable for its substantial potential for carbon absorption on a global scale (~0.02 Gt C yr^{-1}) (Kahl et al., 2017).The emergence of an acidification rate ranging from ~0.001 to ~0.0018 per year in the water masses adjacent to the shelf is likely linked to ongoing CO_2 capture processes. In particular, the northern area of the shelf exhibits the lowest pH values, attributed to the heightened rate of remineralization occurring in the coastal region (Orselli et al., 2018). Biological processes have been identified as primary drivers of carbon capture in the shelf area (Kahl et al., 2017; Schloss et al., 2007), with model predictions indicating that a significant portion of autochthonous biogenic material is exported to the open ocean in subduction zones at the confluence of the Brazil and Malvinas currents (Berden et al., 2020; Franco et al., 2018). Despite the recognition of biological mechanisms mediated by microbial food webs as key contributors to carbon capture in the shelf area, the underlying ecological mechanisms remain insufficiently explored.~~

~~Given that both phytoplankton and bacteria are essential in the processing and accumulation of DOM in the sunlit ocean and that selective grazing upon these groups impact on its subsequent directionality, we conducted dilution experiments to measure growth and grazing of total phytoplankton and bacteria and monitored CDOM and FDOM transformation over the course of the experiments. The aim of this study was to assess the fate of dissolved organic matter (DOM) within the context of naturally occurring ecological interactions between producers (phytoplankton and bacteria) and protistan grazers in two areas of the Patagonian Shelf during spring bloom conditions. The examined areas encompassed both the mid shelf region, characterized by low to moderate productivity, and the shelf break, an upwelling and productive area known for recurrent spring bloom formation. We found that regardless of productivity level, grazers preyed selectively on bacteria and that grazing pressure on bacteria was a primary factor driving the short term accumulation of DOM. Our results contribute to better defining the functional roles of protistan grazers in carbon routing within the ocean.~~

Dissolved organic matter (DOM), the second-largest carbon reservoir in the ocean after dissolved inorganic carbon, is subject to dynamic regulation by physical and biological processes (Spencer et al., 2007). Unveiling the nature and dynamics of DOM is essential for gaining deeper understanding of the biochemical pathways through which carbon circulates in marine ecosystems. The optical properties of DOM serve as a marker for its sources and biological reactivity, with chromophoric DOM reflecting phytoplankton production and fluorescence DOM (FDOM) revealing potential sources and biological and photochemical interactions (Stedmon et al., 2003; Romera-Castillo et al., 2010).

Phytoplankton are primary contributors to DOM, yet processes such as viral lysis and protistan grazing also play substantial roles in shaping its composition and quantity. Protistan grazers not only recycle nutrients and enhance bloom sustainability but also impact carbon cycling through DOM production via biomass reworking and excretion (Kujawinski et al., 2004; Baña et al., 2014; Moran et al. 2022). In addition, grazers influence DOM pools by exhibiting selective feeding behaviors regarding bacterial and phytoplanktonic prey. For example, while size-specific grazing prompt compositional shifts in phytoplankton (e.g., Kanayama et al., 2020), the more generalist grazing on bacteria implies that community structure remains relatively unchanged under grazing pressure (Baltar et al., 2016). On the other hand, grazing on bacteria seems to remain close to

bacterial production, specially under oligotrophic conditions (Sanders et al., 1992), while phytoplankton may temporally scape protistan grazing under favourable growth conditions thus allowing for bloom formation (Irigoien et al., 2005). This results in varying trophic transfer efficiency between phytoplankton- and bacteria-based food webs, with the former typically involving fewer carbon steps before reaching microcrustaceans (Berglund et al., 2007).

The Patagonian Shelf, one of the world's largest continental shelf regions, serves as a hotspot for carbon cycling due to its high productivity and dynamic mixing processes that connect the euphotic zone with bottom sediments (Laruelle et al., 2018). One of its defining features is a 2,500 km-long upwelling front at the shelf break, known for recurrent spring blooms and significant biogeochemical transformations that contribute to global carbon sequestration (Romero et al., 2006; Kahl et al., 2017). The emergence of an acidification trend in the water masses adjacent to the shelf is likely linked to ongoing carbon dioxide (CO_2) capture, especially in the northern area of the shelf (Orselli et al., 2018).

Given the critical roles of phytoplankton and bacteria in DOM processing and the influence of selective grazing, we conducted dilution experiments on the Patagonian Shelf during spring bloom conditions. Our study aimed to assess the fate of DOM by (i) examining the growth and grazing interactions of total phytoplankton and bacteria and (ii) tracking the chromophoric fraction of DOM and FDOM changes over time. The research spanned the mid-shelf (low to moderate productivity) and the highly productive shelf break front. We hypothesized that under conditions of moderate productivity, both bacterial- and phytoplankton-derived carbon are predominantly channeled through protistan grazing, thereby enhancing microbial loop activity. In contrast, in high productivity environments, the reduced efficiency of protists in utilizing phytoplankton biomass facilitates carbon export. We found that protistan grazing selectively targeted bacteria under both productivity regimes, and that intense grazing pressure on bacteria may contribute to the short-term accumulation of DOM substances, irrespective of productivity levels. These findings enhance our understanding of the ecological mechanisms influencing carbon flow in marine ecosystems.

2. Material and Methods

2.1 Sampl~~eing strategy~~collection and analyses

~~The Patagonian Shelf is one of the largest continental shelf areas in the world and its more conspicuous feature is the presence of a 2500 km-long upwelling front at the shelf break area characterized by recurrent spring blooms and intense geochemical transformation (Romero et al., 2006). Biological carbon fixation in this frontal area contributes substantially to the sequestration of large amounts of carbon and constitutes one of the major CO_2 sinks at the global level (Kahl et al., 2017).~~Two groups of stations were selected in the mid-shelf (stations 23, 22 and 21 from the coast to the open ocean) and the shelf break ~~area~~ front (stations 14, 13 and 12 from the coast to the open ocean). Mid-shelf stations were separated by ca. 30 km intercepting the 50 m isobath, while shelf break front stations were separated by ca. 18 km and intercepted the 100 and 200 m isobaths. According to the bioregionalization of the Patagonian shelf waters proposed by Delgado et al. (2023), mid-shelf stations ~~are~~ were located in low to moderate productivity regions (mean chlorophyll-a concentration during the spring peak between 1.14 and 2.48 ~~mg m^{-3}~~ $\mu g\ L^{-1}$), while the shelf break front stations ~~are~~ were nested in the upwelling,

highly productive region (mean chlorophyll-a concentration during the spring peak of 5.8 $\mu g\ L^{-1}$~~$mg\ m^{-3}$~~). Hydrographic data (temperature, salinity, pressure, and fluorescence) were taken with a CTD profiler SBE 9plus during the cruise H0917 from October 9 to 12, 2017.

Water samples for dissolved nutrients and for running the experiments were taken from the chlorophyll-a maximum with 6 L Niskin bottles attached to the CTD rosette, while dissolved organic carbon (DOC) samples were taken in the surface layer (5 m). The measurement of inorganic nutrients (NO_2^-, NO_3^- and NH_4^+, PO_4^{3-}, and Si), was carried out by analyzing 50 mL aliquots of seawater preserved with $HgCl_2$ solution (Kattner and Becker, 1991). The concentration of dissolved inorganic nitrogen (DIN) was calculated as the sum of NO_2^-, NO_3^- and NH_4^+. Filtered (Whatman GF/F glass fiber filters) samples for DOC were collected in pre-combusted 20 mL glass vials and acidified to pH < 2 with H_3PO_4. Filtrates were analyzed using high-temperature (680°C) catalytic oxidation with Al_2O_3 particles containing 0.5% platinum (Pt) in a TOC analyzer (Dohrmann DC-190, CA, USA). The resulting CO_2 was then quantified using non-dispersive linearized infrared gas analysis (Skoog et al., 1997).

~~**2.2 Analytical determination of inorganic nutrients and DOC**~~

~~Water samples for chemical/plankton determinations and experiments, were taken from the chlorophyll-a maximum with 6 l Niskin bottles attached to the CTD rosette, while dissolved organic carbon (DOC) samples were taken in the surface layer (5 m). Water samples aliquots were taken for the analysis of dissolved nutrients. The measurement of inorganic nutrients ($NO_2^=$, $NO_3^=$ and NH_4^+, PO_4^{3-}, and Si) was carried out by analyzing 50 ml aliquots of seawater preserved with $HgCl_2$ solution (Kattner and Becker, 1991) The concentration of dissolved inorganic nitrogen (DIN) was calculated as the sum of $NO_2^=$, $NO_3^=$ and NH_4^+. Filtered (pre-combusted Whatman GF/F glass fiber filters) samples for DOC were collected in pre-combusted 20 ml glass vials and acidified to pH < 2 with H_3PO_4. Filtrates were analyzed using high-temperature (680°C) catalytic oxidation with Al_2O_3 particles containing 0.5% platinum (Pt) in a TOC analyzer (Dohrmann DC-190, CA, USA). The resulting CO_2 was then quantified using non-dispersive linearized infrared gas analysis (Skoog et al., 1997). Potassium hydrogen phthalate solution was used as the calibration standard.~~

~~2.3~~2.2 Satellite chlorophyll-a

The spring phytoplankton bloom is a recurrent feature of the Patagonian Shelf and shelf break (e.g., Delgado et al., 2023). A time series of satellite-derived chlorophyll-a was constructed to capture the bloom timing at each station during the sampling period. Moderate Resolution Imaging Spectroradiometer (MODIS) Aqua images of chlorophyll-a concentration were downloaded from the National Aeronautics and Space Administration (NASA) ocean color web site (https://oceancolor.gsfc.nasa.gov/). Daily Level 3~~ (L3)~~ images with a spatial resolution of 4 km were obtained for the period spanning August 2017 to December 2017, capturing the closest pixel to each sampling point. ~~These images were utilized to construct time series data for each station and assess the phytoplankton's growth phase at each location.~~ To minimize the percentage of missing values, we computed the 5-day mean and applied a low-pass filter to remove the variability lower than 28 days.

~~2.4~~2.3 Experimental set-up

Feeding experiments, based on the dilution technique (Landry and Hassett, 1982), were prepared by gently mixing different ~~amounts~~ percentages of unfiltered water and filtered water through <0.2 µm ~~water (using~~ Whatman polycarbonate filters~~) in acid-cleaned glass bottles (1 l)~~. Four dilution treatments (D) were prepared using the filtered and unfiltered water: 10%, 40%, 70% and 100% (whole water). ~~An additional treatment consisting of filtered seawater (<0.7 µm, using Whatman GF/F glass fiber filters) was set to evaluate chromophoric (CDOM) and fluorescent dissolved organic matter (FDOM) modifications in the absence of protists and grazers. Seawater~~ Water ~~from each site was obtained from the chlorophyll-a maximum (20-30 m depth), and~~was pre-filtered by a 200 µm mesh net to eliminate larger, metazoan grazers. Acid-cleaned, 1 L glass ~~Experimental~~ experimental bottles (3 replicates) were daily (24 h) deployed at a deck-incubator (200 ~~l~~L) equipped with continuous in situ water flow and covered with a double knitted mesh fabric (~215 g m^2) to attenuate the UV radiation. Dissolved inorganic nutrients (N, P and Si) were added to the incubation bottles following the recommendations by Calbet and Saiz (2018) to ensure phytoplankton growth at non-limiting conditions. Assuming moderate phytoplankton growth rates and maximum chlorophyll-a concentrations of 2 µg L^{-1} in the mid-shelf region and 6 µg L^{-1} in the shelf break front (Delgado et al., 2023), we supplemented the water with 8.3 µM of nitrogen and silicon, and 0.5 µM of phosphorus in the mid-shelf area, and 24.9 µM of nitrogen and silicon, and 1.5 µM of phosphorus in the shelf break front~~by assuming a maximum chlorophyll-a concentration in the mid-shelf area of 2 µm l^{-1} (Delgado et al., 2023), and in the shelf-break area of 10 µm l^{-1}. The amount of nutrients added followed the recommendationsCalbet and Saiz (2018) to ensure phytoplankton growth at non-limiting conditions~~. A series of triplicate dilution bottles without added nutrients ~~addition~~ was set as control treatment.

Subsamples from the initial and final treatments were collected for chlorophyll-a and bacteria abundance analyses. To determine chlorophyll-a, samples (300 mL) were filtered through Whatman GF/F glass fiber filters and stored at -20°C. Pigments were extracted with 90% acetone for 24 h in the dark at -20° C and then determined spectrophotometrically according to Jeffrey and Humphrey (1975). Heterotrophic bacteria were quantified by staining 1 mL seawater sample with 4,6-diamidino-2-phenylindole (DAPI) to a final concentration of 3 µg mL^{-1} and collected on black polycarbonate filters (25 mm diameter, 0.2 µm pore size). The enumeration was done with a Nikon Eclipse 80i microscope equipped with a fluorescence lamp at 100X magnification and using a UV excitation filter (330-385 nm). Twenty-five images were taken at random points from each polycarbonate filter using a Nikon DXM1200F digital camera and subsequently, every cell in the image was enumerated and sized using the software ImageJ. Bacterial cell volumes were calculated assigning simple geometric shapes to species (coccos, bacillus), and converted into carbon content (µg C L^{-1}) by the allometric model according to Simon and Azam (1989).

Plankton samples were collected from the initial treatments to characterize the community structure at the starting conditions. For the analysis of plankton in the 2–5 µm size range, triplicate samples (3 mL) were fixed with 0.53 mL of glutaraldehyde (f.c. 2 %) and subsequently processed following the methods described by Porter and Feig (1980). The same procedure was applied for plankton in the 5–20 µm size range, using duplicate 100 mL samples for counting. The identification of organisms was done by a combination of light and epi-

fluorescent microscopy. Preserved samples were stained with DAPI (f.c. 5 µg mL^{-1}) and proflavine (f.c. 5 µg mL^{-1}) and collected on black polycarbonate filters (25 mm diameter, 0.2 µm pore size). Most taxa were identified using a blue excitation filter (450-490 nm) while Cryptophytes were identified using a green excitation filter (480-550 nm). Cell enumeration was done by settling the preserved sample (1-2 mL) in Utermöhl chambers during 24 h. The entire chamber was analyzed under a Wild M20 inverted light microscope. Similarly, the enumeration of plankton in the size fraction 20-200 µm was done by settling a variable volume (50–100 mL, depending on sediment and plankton concentration) of preserved water sample (Lugol's iodine) in Utermöhl chambers during 24 h. It is worth mentioning that since samples were pre-filtered through a 200 µm mesh to exclude larger consumers from our experiments, colony-forming protists may have been removed. Biomass estimation involved assigning simple geometric shapes to species to quantify cell volume, which was subsequently converted into carbon content (µg C L^{-1}) according to Hillebrand et al. (1999). ~~Simon and Azam (1989)~~

Protistan taxa abundance was visualized by a heatmap (employing the R package *heatmaply*). Heterotrophic and autotrophic taxa were segmented into groups based on size, distinguishing between nanoplankton (2-20 µm) and microplankton (20-200 µm) (Sieburth et al., 1978). Nanoplankton included heterotrophic nanoplankton (HNP), coccolithophores, and phototrophic nanoplankton (PNP), while the microplankton comprised ciliates, heterotrophic dinoflagellates (HD), phototrophic dinoflagellates (PD), and diatoms. ~~(Sieburth et al., 1978)~~Additionally, HNP comprised both flagellates and ciliates, while PNP encompassed dinoflagellates, diatoms, and flagellates. A side dendrogram was included to group similar sampling stations by ordering rows (stations) so that the sum of distances between each one will be minimized. Data for ranking rows was normalized to range from 0 to 1. To identify the dominant taxa contributing to station ordination, a biplot based on non-metric Multi-Dimensional Scaling (MDS) was created using the R package *vegan*.

An additional treatment of pre-filtered (Whatman GF/F glass fiber filters) and undiluted water was set to separate protists and measure the absorbance at 254 nm and FDOM. This was aimed to compare the DOM pool at the initial and final incubation conditions in the presence (i.e., in unfiltered, undiluted treatment) and in the absence of protists (i.e., in pre-filtered by 0.7 µm, undiluted treatment). Biotic effects are known to produce DOM transformations in short timescales. For instance, ~~(Timko et al., 2015)~~significant shifts in both the chromophoric and fluorescent fractions of DOM driven by biological processes were identifiable after 24 h (Urban-Rich et al., 2004; Lønborg et al., 2010~~;~~ 2015~~; Urban-Rich et al., 2004~~), while DOM transformation driven by bacteria occurred within the first 24 h upon their release by phytoplankton (Gruber et al., 2006; Hach et al., 2020).

The optical properties of FDOM were evaluated from emission-excitation matrices (EEM) obtained with a Shimadzu RF-5301 scanning spectrofluorometer with a 150 W xenon lamp and a 1 cm quartz cell. Milli-Q water was used as reference and the intensity of the Raman peak was regularly checked. The emission wavelength ranged between 250 nm and 600 nm while the excitation wavelength ranged between 220 nm and 370 nm. Dissolved humic-like and protein-like substances were estimated using the wavelengths proposed by Coble (1996). Humic-like material was represented by three fluorophores: $FDOM_C$ (Ex/Em: 350/440) and $FDOM_A$ (Ex/Em: 250/425) of terrestrial origin, and $FDOM_M$ (Ex/Em: 310/380) of marine origin. $FDOM_C$

indicates highly unsaturated components, $FDOM_A$ reflects a moderate degree of unsaturation, and $FDOM_M$ suggests a low degree of unsaturation. Protein-like material was characterized by two fluorophores: $FDOM_B$ (Ex/Em: 260/300) and $FDOM_T$ (Ex/Em: 270/330), both derived from autochthonous biogenic sources. $FDOM_B$ is associated with compounds similar to tryptophan and tyrosine, linked to recent organic matter production through primary productivity, while $FDOM_T$ indicates tryptophan-like compounds formed from microbial protein breakdown (Jørgensen et al., 2011; Drozdova et al., 2022). Fluorescence intensity of fluorophores was expressed in Arbitrary Units (AU). Fluorophores were identified using the PARAFAC multivariate algorithm (Stedmon and Bro, 2008), and different biogeochemical indicators such as humification index (HIX), fluorescence index (FI), and freshness index (BIX), were calculated (Coble, 1996). The HIX serves as a tool for assessing the diagenetic condition of DOM, as it increases with aromaticity (Bai et al., 2015), while the FI distinguishes between DOM of different origins, i.e., terrestrial vs. microbial (McKnight et al., 2001). The BIX aims to estimate the relative contribution of DOM produced in situ by microbes (Huguet et al., 2009).

The absorbance spectra between 240 to 800 nm were measured in a Perkin Elmer Lambda 35 spectrophotometer. The absorbance at 254 nm (a254) from the chromophoric fraction of DOM was used as a proxy of the DOM amount (Brandstetter et al., 1996). Net changes in the a254 fraction of DOM across the incubation time were calculated as 1/t ln (a254)t/(a254)0, where (a254)0 and (a254)t are the a254 nm at the initial (0) and final (t) conditions, respectively. Lee et al. (2018) identified parameters with more than a 50% absolute percent difference between the control and treated samples as reliable indicators to distinguish between DOM transformation caused by biodegradation, UV irradiance, and adsorption. Here we used the tendency during incubation of BIX, HIX, FI, and the ratio between FDOM components M and A ($FDOM_M/FDOM_A$) as reliable parameters for the discrimination of biodegradation versus UV photodegradation or adsorption. Pairwise relationship between net changes in a254 in the presence and absence of protists with variables of interest, was evaluated by simple regression models. The same procedure was used with other variables to test for pairwise relationships of ecological significance.

~~2.5~~2.4 Phytoplankton and bacterial growth and grazing by phagotrophic protists

Rate estimates of phytoplankton growth (μ) and mortality due to protist ~~phagotrophy~~ grazing (m) were obtained using the equations of Landry and Hassett (1982). While initially intended for measuring phytoplankton growth and mortality, we adapted this method to assess bacterial growth rate and bacterivory. This approach has been demonstrated to be effective and reliable for use with natural bacterial communities in non-oligotrophic regions (Tremaine and Mills, 1987). The method is based on measuring the initial and final concentration of chlorophyll-a (as a proxy of phytoplankton biomass) and bacterial abundance in triplicate dilution series after an incubation period of 24 h. It assumes that protistan grazing rate is a linear function of prey concentration (Holling type I functional response), and can be calculated as follows:

$$\mu_0 = 1/t \ln Pt/P0 = \mu - mD$$

where μ_0 is the apparent growth rate, P0 and Pt are the phytoplankton concentration at the initial (0) and final (t) conditions, respectively, D is the dilution series. The m:μ ratio x 100 was used to calculate the percentage of the daily bacterial/primary productivity consumed by protistan grazers. We tested model fit by linear regression analysis in every experiment.

~~**2.6 Plankton abundance and biomass**~~

~~Subsamples from the initial and final treatments were collected for chlorophyll-a and bacteria abundance analysis. To determine chlorophyll-a, triplicate samples (300 ml) were filtered through GF/F filters and stored at -20°C. Pigments were extracted with 90% acetone for 24 h in the dark at -20° C and then determined spectrophotometrically according to Jeffrey and Humphrey (1975). Triplicate samples of picoplankton (3 ml) and duplicate samples of nanoplankton (100 ml) were fixed with 0.53 ml of glutaraldehyde (f.c. 2 %) and subsequently processed following the methods described by Porter and Feig (1980). Hillebrand et al. (1999)Heterotrophic bacteria were quantified by staining 1 ml seawater sample with 4,6 diamidino 2-phenylindole (DAPI) to a final concentration of 3 μg ml^{-1} and collected on black polycarbonate filters (25 mm diameter, 0.2 μm pore size). The enumeration was done with a microscope Nikon Eclipse 80i equipped with a fluorescence lamp at 100X magnification. Heterotrophic bacteria were identified using a UV excitation filter (330-385 nm). Twenty-five images were taken at random points from each polycarbonate filter using a Nikon DXM1200F digital camera and subsequently, every cell in the image was enumerated and sized using the software ImageJ. Bacterial cell volumes were calculated assigning simple geometric shapes to species (coccos, bacillus), and converted into carbon content (μg C l^{-1}) by the allometric model according to Simon and Azam (1989).~~

~~Protist plankton identification and quantification were conducted using light and epi-fluorescence microscopy at the initial treatment stage. The identification of photosynthetic (PNP) and heterotrophic nanoplankton (HNP) was done by a combination of light and epi-fluorescent microscopy. Note that the size categories PNP and HNP include members from nanoplankton (5-20 μm) and ultraplankton (>5 μm). Prior to cell enumeration, preserved samples (5 ml) were stained with DAPI (f.c. 5 μg ml-1) and proflavin (f.c. 5 μg ml-1) and collected on black polycarbonate filters (25 mm diameter, 0.2 μm pore size). Most PNP and HNP were identified using a blue excitation filter (450-490 nm) while Cryptophytes were identified using a green excitation filter (480-550 nm). Cell enumeration was done by settling the preserved sample (1-2 ml) in Utermöhl chambers during 24 h. The entire chamber was analyzed under a Wild M20 inverted light microscope. Similarly, the enumeration of phytoplankton and phagotrophic protists in the size fraction 20-200 μm was done by settling a variable volume (10-50 ml, depending on sediment and plankton concentration) of preserved seawater sample (Lugol's iodine) in Utermöhl chambers during 24 h. It is worth mentioning that samples were pre-filtered through a 200 μm mesh to exclude larger consumers from our experiments. This procedure may have also removed colony-forming protists. Biomass estimation involved assigning simple geometric shapes to species to quantify cell volume, which was subsequently converted into carbon content (μg C l^{-1}) according to Hillebrand et al. (1999). Protistan taxa abundance was visualized by a heatmap (employing the R package *heatmaply*), and taxa was segmented into (Sieburth et al., 1978)functional groups to facilitate visualization. A side dendrogram was~~

included to group similar sampling stations by ordering rows (stations) so that the sum of distances between each one will be minimized. Data for ranking rows was normalized to range from 0 to 1. To assess the dominant taxa contributing to station ordination, a biplot based on non-metric Multi-Dimensional Scaling (MDS) was done to evaluate the correlation of taxa on the station ordination using the R package *vegan*.

2.7 Production of CDOM and FDOM transformation

Given that protistan grazing impacts on carbon pools, either by remineralizing organic carbon or by contributing with the formation of DOM by reworking phytoplankton and bacterial biomass (Baña et al., 2014; Lund Paulsen et al., 2019), and that these processes add to the isolated effects of phytoplankton growth and bacterial degradation of DOM in natural communities, we estimated the net DOM production and evaluated the fate of biodegradable and biorefractory compounds during the incubations. For this purpose, we measured CDOM and FDOM at the beginning and end of the experiments in the presence (undiluted treatment, prefiltered by 200 µm) and absence of protists (undiluted treatment, prefiltered by 0.7 µm). This procedure captured transformation processes within closed systems at the daily basis. Many biotic and abiotic transformation processes occur at the daily timescale. For instance, photodegradation of refractory products occurs within hours (Timko et al., 2015), while experimental observations revealed that significant shifts driven by biological processes were identifiable after 24 h (Lønborg et al., 2010, 2015; Urban-Rich et al., 2004). Furthermore, experimental results revealed that major microbially driven DOM transformation occur within the first 24 h upon their release by phytoplankton (Gruber et al., 2006; Hach et al., 2020). This emphasizes that detectable DOM transformation processes occurring at short term periods, can provide clues to assess transient DOM trends within specific succession phases of microbial communities. It is worth mentioning that the treatment filtered by 0.7 µm, excluded part of the bacterioplankton community, notably the particle-attached bacteria, and thus may not accurately reproduce the response of natural communities.

The optical properties of FDOM were evaluated from emission-excitation matrices (EEM) obtained with a Shimadzu RF-5301 scanning spectrofluorometer with a 150W xenon lamp and a 1 cm quartz cell. Milli-Q water was used as reference and the intensity of the Raman peak was regularly checked. The emission wavelength ranged between 250 nm and 600 nm while the excitation wavelength ranged between 220nm and 370nm. An estimation of dissolved humic-like and protein-like substances was carried out at the wavelengths proposed by Coble (1996). Humic-like fluorophores: $FDOM_C$, containing mostly highly unsaturated components, at Ex/Em: 350/440 nm; $FDOM_A$, with moderate degree of unsaturation, at Ex/Em: 250/425 nm and $FDOM_M$, with low degree of unsaturation, at Ex/Em:310/380 nm. Protein-like fluorophores: $FDOM_T$, with fresh components, at Ex/Em: 270/330 nm and $FDOM_B$, corresponding to DOM transformed by biological or physicochemical factors, at Ex/Em: 260/300 nm. Fluorescence intensity of fluorophores was expressed in Arbitrary Units (AU). Fluorophores were identified using the PARAFAC multivariate algorithm (Stedmon and Bro, 2008) and different biogeochemical indicators such as humification index (HIX), fluorescence index (FI), and freshness index (BIX), were calculated (Coble, 1996). The HIX serves as a tool for assessing the diagenetic condition of DOM, as it increases with aromaticity (Bai et al., 2015), while the FI distinguishes between DOM of different

~~origins, i.e., terrestrial vs. microbial (McKnight et al., 2001). BIX aims to estimate the relative contribution of DOM produced in situ by microbes (Huguet et al., 2009).~~

~~CDOM was measured as the absorbance spectra between 240 to 800 nm measured in a Perkin Elmer Lambda 35 spectrophotometer. The absorbance at 254 nm (a254) was used as a proxy of total DOM in the UV spectrum (Brandstetter et al., 1996). Net DOM production was calculated as 1/t ln (a254)t/(a254)0, where (a254)0 and (a254)t are the absorbance at 254 nm of CDOM at the initial (0) and final (t) conditions, respectively. Lee et al. (2018) identified parameters with more than a 50% absolute percent difference between the control and treated samples as reliable indicators to distinguish between DOM transformation caused by biodegradation, UV irradiance, and adsorption. Here we used the tendency during incubation of BIX, HIX, FI, and the ratio between FDOM components M and A ($FDOM_M/FDOM_A$) as reliable parameters for the discrimination of biodegradation versus UV photodegradation or adsorption. Pairwise relationship between net production of DOM in the presence and absence of protists with variables of interest, was evaluated by simple regression models. The same procedure was used with other variables to test for pairwise relationships of ecological significance.~~

3. Results

3.1 Phytoplankton phenological stages at the sampling area

Mean surface chlorophyll-a, derived from satellite observations during the sampling period (October 9-12, 2017, Fig. 1a), revealed a band of high phytoplankton concentration at the shelf break front, centred at the 114 m isobath in the latitudinal band at 40°S. While the spring bloom typically begins during September in the latitudinal range of our sampling area (Delgado et al., 2023), phytoplankton at the time of sampling, as estimated from satellite chlorophyll-a, were at different phenological stages in each station (Fig. 1b). At the mid-shelf, station 21 showed the highest concentration of satellite chlorophyll-a and the phytoplankton community was at the pulse initiation. Stations 22 and 23 showed lower chlorophyll-a and were sampled at bloom stationary phase. At the shelf break front, satellite-derived chlorophyll-a levels were elevated in stations 13 and 14, indicating proximity to the bloom peak, whereas station 12 exhibited low chlorophyll-a concentration~~s~~, corresponding to the bloom termination phase.

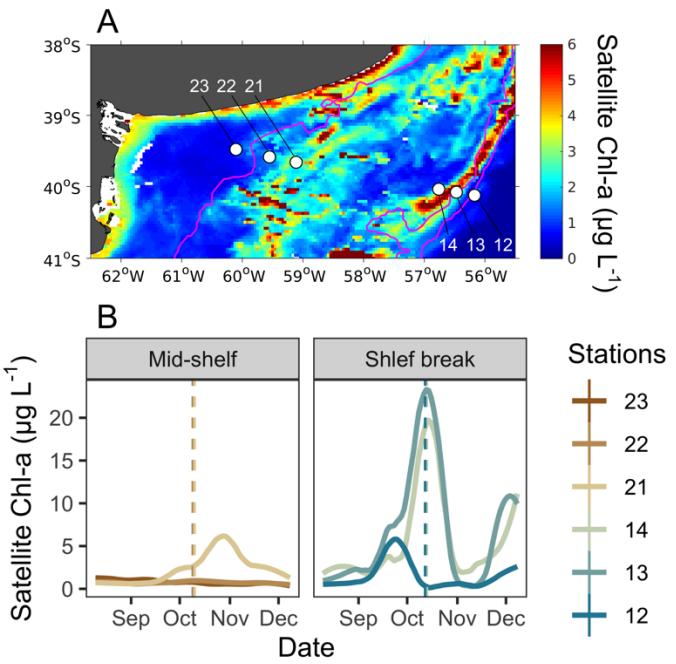

Figure 1.A. Map of the study site showing the location of sampling stations (white dots) and the mean surface distribution of satellite chlorophyll-a (Chl-a) ~~(MODIS-AQUA)~~ during the sampling period (October 09-12). Stations 23, 22 and 21 were located in the mid-shelf area, and stations 14, 13 and 12 were located in the shelf break front. B. Temporal evolution of surface satellite ~~chlorophyll-a~~Chl-a concentration at grid points closest to sampling stations in the mid-shelf and the shelf break front. Solid lines denote satellite ~~chlorophyll-a~~Chl-a concentration at each station, while ~~dotted~~ dashed lines represent the ~~moment~~ date of in situ sampling. Lines are color-coded according to the ~~points~~ symbols representing each station.

3.2 Hydrography, nutrients, and DOM properties

Thermohaline signature was in the range of the Subantarctic Shelf waters (33.5 < S < 34) from station 21 to station 14 in agreement with Berden et al. (2020) and Ferronato et al. (2023). At the mid-shelf area, station 23 and 22 showed relatively higher salinity ~~water~~ values (S > 33.7), linked to the coastal maximum salinity waters originating~~d~~ at San Matias Gulf (Lucas et al., 2005). These stations also showed weak stratification, while the rest of the stations showed a sharper thermocline. The mixed layer depth (MLD) ~~ranged between~~was shallower (10 m) in ~~10 (~~stations 12 and 23, whereas in all other stations, it averaged 30 m.~~) and 31 m (stations 13 and 22). Stations 14 and 21 showed intermediate MLD of 30 and 28 m respectively.~~ All samples taken at the chlorophyll-a maximum were positioned within the mixed layer.

The concentration of dissolved nutrients (DIN, PO_4^{3-} and Si) was highest at station ~~14~~ 12, while the lowest~~s~~ total nutrient concentration was recorded at station 23 (Fig. 2~~a~~). The primary nitrogen source was NO_3^-, except for station 22 where NH_4^+ predominated. The only notable distinction between station groups was the concentration of NO_3^-, which averaged 1.2 µM in the mid-shelf stations and 7.3 µM in the shelf ~~-~~break front

stations. According to Redfield ratios (Redfield et al., 1963), a strong nitrogen depletion in relation to PO_4^{3-} and Si occurred in station 23. While the N:P ratio was closer to 16:1 in the rest of the stations, a general excess of PO_4^{3-} in relation to DIN was registered. On the contrary, all stations except for station 23, showed a Si depletion in relation to DIN. The concentration of DOC in surface waters was homogeneous in the mid-shelf stations (mean of 79 µM), while in the shelf break it varied from 96 µM, in station 14, to 52 µM, in station 13 (Fig. 2~~b~~). The highest fluorescence intensity of protein-like compounds ($FDOM_T$ and $FDOM_B$) was found in station 23, while the highest intensity of humic-like fluorophores was observed in station 21 (Fig. 3). The a254 was higher in the mid-shelf stations (mean of 2.3 m^{-1}) compared to the shelf break front stations (mean of 1.3 m^{-1}).

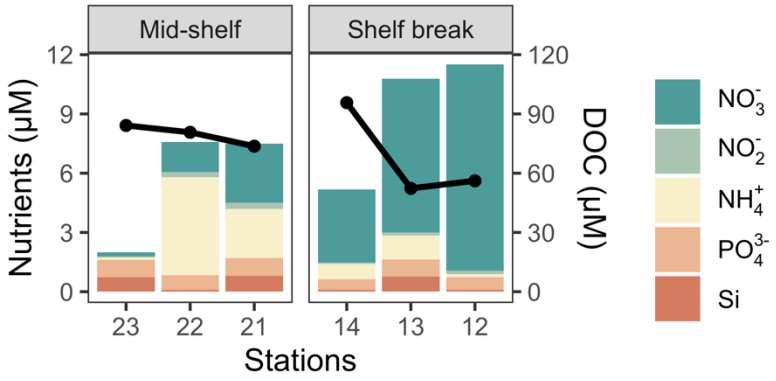

Figure 2. Cumulative nutrient concentrations at the deep chlorophyll-a maximum (bars) and the concentration of DOC in surface waters (solid black line) across stations in the mid-shelf and the shelf break front.

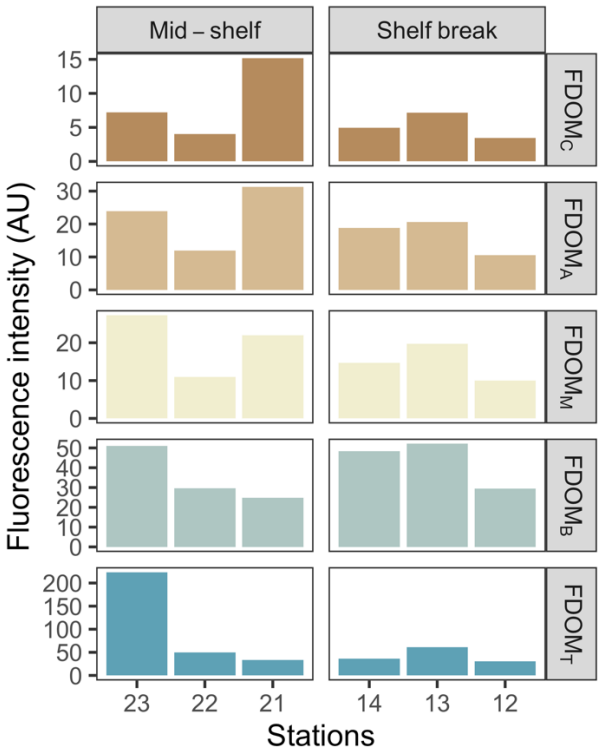

Figure 3. Fluorescence intensity of main identified FDOM components at the deep chlorophyll-a maximum across stations in the mid-shelf and the shelf break front. FDOM components are shown in a decreasing order of humification from top to bottom plots.

3.3 Plankton community structure

The biomass of protistan grazers exceeded that of phytoplankton and heterotrophic bacteria at most sampling stations, except at stations 13 and 14, where phytoplankton biomass dominated (Fig. 4a). ~~The type of food web structure based on the ranking of the carbon biomass of phagotrophs, phytoplankton and heterotrophic bacteria, and the spatial distribution of these groups' biomass are shown in Fig. 4a and b,~~ Heterotrophic dinoflagellates dominated the biomass across stations, except at station 14, where HNP prevailed. In contrast, no clear distribution pattern was observed among phytoplankton groups~~respectively~~. Biomass of heterotrophic bacteria ranged between 2.6 (station 22) and 15 µg C ~~l~~L^{-1} (station 14) (Fig. 4b). The abundance of this group was positively associated with chlorophyll-a concentration (R^2=0.7, p=0.04) and the abundance and biomass of most phytoplankton groups (p<0.05), except coccolithophores. The highest bacterial abundance and biomass was registered under chlorophyll-a pulse initiation (stations 21, 13 and 14). Among ~~phagotrophic~~ protist~~an~~s grazers, the most significant group in terms of biomass were dinoflagellates ranging from 0 (station 14) to 134 µg C ~~l~~L^{-1} (station 22, mostly due to the presence of *Noctiluca scintillans*). Ciliates ranged from 0 (station 14) to 20 µg C ~~l~~L^{-1} (station 21), while HNP showed the highest biomass in stations 13 and 14 (5 and 6 µg C ~~l~~L^{-1}, respectively), and the lowest value was registered in station 12 (0.6 µg C ~~l~~L^{-1}). ~~Ultrazooplankton~~ Plankton <5 µm (choanoflagellates and other unidentified flagellates) was the dominant fraction among HNP except in station

13, were micro-sized ciliates and nano-sized flagellates (*Telonema* sp. and unidentified dinoflagellates) dominated biomass.

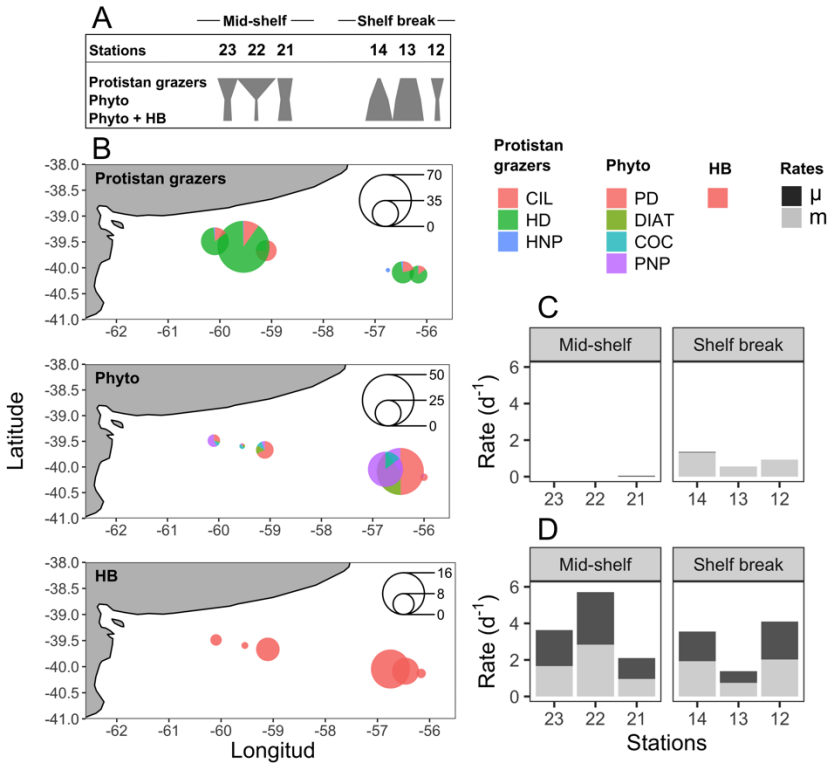

Figure 4.A. Polygons represent the ~~Type~~ type of food web structure based on the ranking of carbon biomass of ~~phagotrophs~~protistan grazers, phytoplankton (phyto), and heterotrophic bacteria (HB) in each sampling station (indicated above the polygons). Inverted or top-heavy pyramids (stations 23, 22, 21 and 12), occur when the biomass of protistan grazers surpasses that of their prey (phytoplankton plus HB). In contrast, the more conventional bottom-heavy structure (stations 14 and 13), are characterized by a greater prey biomass relative to that of consumers. B. Spatial distribution of the cumulative biomass (μg C ~~l~~L^{-1}) of ~~phagotrophs~~ protistan grazers (upper plot), phytoplankton (mid-plot) and HB (lower plot). Scale circles are shown within each plot. C. Growth (μ) and grazing (m) rates of phytoplankton. D. Growth (μ) and grazing (m) rates of HB.

~~Whitin phytoplankton, four main groups were identified: photosynthetic nanoplankton (PNP, including photosynthetic nanoflagellates, nano sized diatoms and dinoflagellates), micro sized photosynthetic dinoflagellates (PD), micro sized diatoms, and coccolithophores.~~ The biomass of photosynthetic taxa was generally dominated by PNP ~~generally dominated the biomass of photosynthetic taxa~~. The highest concentration and biomass of all groups, except for coccolithophores, was registered in station 13 (PNF: 32 μg C ~~l~~L^{-1}, PD: 8 μg C ~~l~~L^{-1}, diatoms: 6 μg C ~~l~~L^{-1}). High biomass of PNP and dinoflagellates was also registered in station 14 (34

µg C ~~l~~L^{-1}) and station 21 (8.5 µg C ~~l~~L^{-1}), respectively. The highest biomass of coccolithophores was registered in station 22 (2 µg C ~~l~~L^{-1}).

Stations 12 and 13 showed ~~conspicuous~~ differences on microplankton community structure compared to the rest of the stations (Fig. 5). According to the ordination fit between vectors (i.e., taxa) and stations, the ~~phagotrophic~~ protistan grazers ~~species~~ that mainly contributed to separate these two stations from the others were the dinoflagellates *Gymnodinum* spp., and *Protoperidinium pellucidum*, while *Pyramimonas* sp. and *Dinophysis acuminata*, were the distinctive photosynthetic species in these stations (MDS, $p<0.05$). Stations 22 and 23 were also closely associated regarding the ~~heterotrophic~~ protistan grazers community and the species that contributed most to this association was *Strombidinopsis* sp.

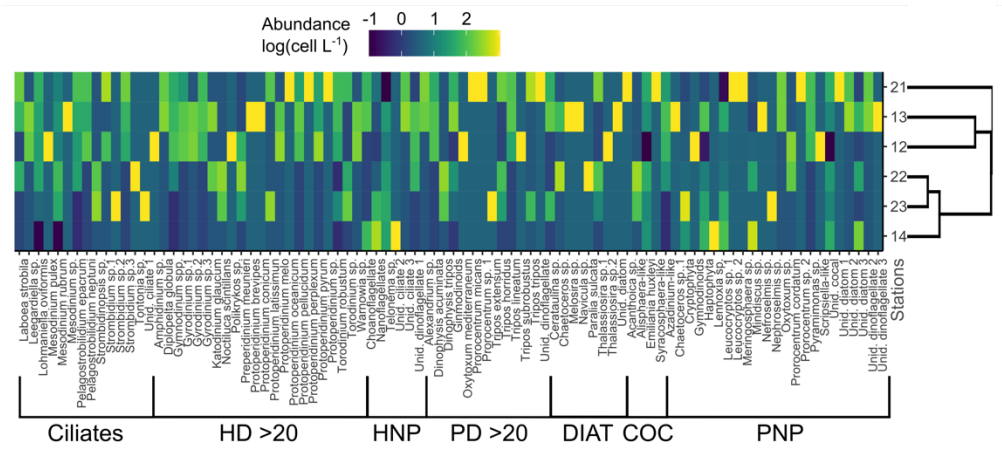

Figure 5. Color-coded, log-transformed cell abundance (cell ~~l~~L^{-1} × 10^3) of plankton taxa (columns) at the sampling stations (rows). ~~Functional g~~Groups ~~delimitation~~ is indicated ~~in~~ at the bottom. Side dendrogram shows the optimal ordering of rows (stations) so that the sum of distances between each one is minimized. HD>20: Heterotrophic dinoflagellates >20 µm, HNP: Heterotrophic nanoplankton, PD>20: Photosynthetic dinoflagellates >20 µm, Diat: Diatoms, Coc: Coccolithophores, PNP: Photosynthetic nanoplankton.

3.4 Growth and grazing rates

Water temperature of the incubator container was hourly monitored and ranged between 12.2 and 13.8°C in the mid-shelf stations and between 8 and 11.1°C in the shelf break stations. Bacteria showed active growth during all experiments while phytoplankton only revealed significant growth rates in conditions of pulse initiation (stations 21 and 14). Some degree of nutrient limitation was detected in the mid-shelf stations as the growth rate of phytoplankton at the control treatments was lower than in the nutrient amended treatment, however, differences were not statistically significant. No apparent differences were found in stations 12, 13 and 14. Significant grazing effect on bacteria was found in all experiments (Fig. 4c), while grazing on phytoplankton was only significant in the shelf break stations (Fig. 4d). In the mid-shelf stations, daily bacterial productivity consumed by HNP averaged 72%, while in the shelf break stations, it reached 83%. Mean daily primary

productivity consumed by ~~phagotrophic protists~~ protistan grazers was zero in the mid-shelf stations and 155% in the shelf break. Linear responses were found in all experiments, indicating that no cascading effects, saturating feeding ~~and~~ or starvation occurred within incubation bottles. The abundance of heterotrophic bacteria was negatively correlated with the grazing of HNP (R^2=0.8, p=0.016) and growth (R^2=0.9, p=0.005).

3.5 Short-term DOM transformations

An accumulation of the a254 DOM fraction ~~accumulation~~ was observed in stations 22, 14, 13, and 12 during the incubation period in the experimental setting with protists, while stations 23 and 21 exhibited DOM consumption (Fig. 6a). Conversely, in the experimental setting without protists, the a254 DOM fraction accumulated in stations 22, 21, 14, and 12, while stations 23 and 13 showed DOM consumption (Fig. 7a). Regardless of net DOM production, biodegradation of organic matter occurred in most experiments as denoted by the decrease ~~of~~ in the BIX and the increase ~~on~~ in the HIX (Fig. 6b, 7b). The prevalence of biodegradation over UV photodegradation or adsorption was further supported by most source discrimination indices (FI and M/A, data not shown). The decrease ~~on~~ in BIX was coherent with the net zero to low phytoplankton growth during our experiments. An exception to this general pattern occurred in station 13, in which HIX increased and BIX decreased during the incubation. Station 13 was characterized by the highest abundance of micro-sized phytoplankton (diatoms and photosynthetic dinoflagellates) and registered the lowest concentration of DOC (52 µM) at the moment of sampling. While HIX and BIX indices suggested that DOM modifications are not driven by biodegradation, M/A decreased and FI increased during the experiments, thus giving inconsistent results.

Among treatments, a shift from ~~DOM~~ accumulation to consumption of the a254 DOM fraction was registered in stations 21 and 13. In the presence of protists, the net a254 fraction of DOM ~~production~~ change was negatively associated with the fluorescence intensity of peaks related to humic-like compounds ($FDOM_C$: R^2=0.6, p=0.07, $FDOM_A$, R^2=0.8, p=0.01, $FDOM_M$: R^2=0.7, p=0.04), and positively associated with the grazing on HB (R^2=0.7, p=0.00, ~~)~~Fig. 8a). In the absence of protists, the net a254 fraction of DOM ~~production~~ change was negatively associated with the ratio between bacteria and phytoplankton biomass (R^2=0.9, p=0.01, ~~)(~~Fig. 8b).

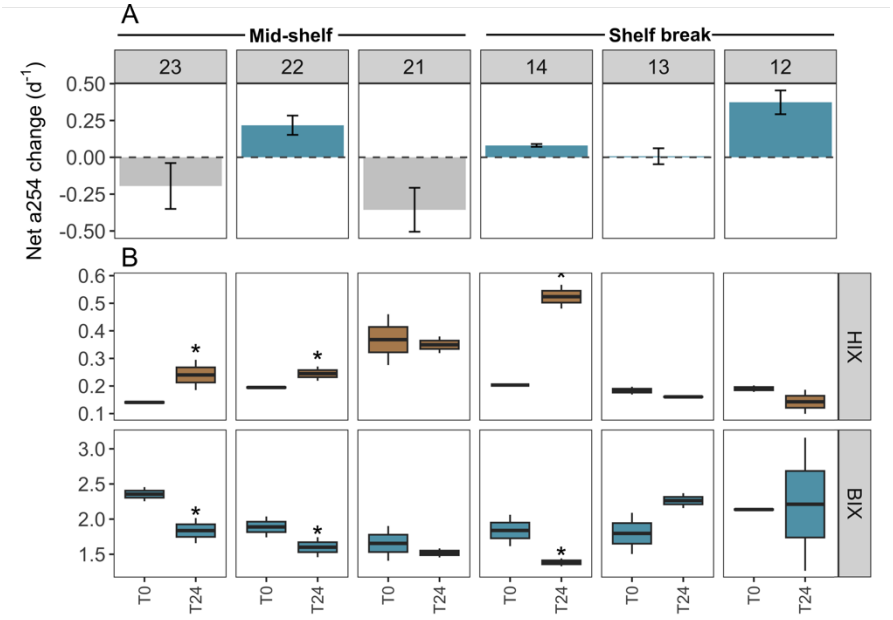

564

565 **Figure 6. DOM transformations in the experimental setting with protists (pre-filtered by 200 µm) across**
566 **stations in the mid-shelf and the shelf break front. A. Net changes in the absorbance at 254 nm (a254)**
567 **from the chromophoric fraction of DOM ~~production as depicted by the absorbance intensity at 254 nm~~,**
568 **a proxy of total DOM concentration. Dashed line indicates the limit between negative (~~net DOM~~i.e.,**
569 **consumption) ~~(negative values)~~ and positive net a254 changes (i.e., ~~net DOM~~ accumulation ~~(positive**
570 **values~~) during the incubation period. B. Shifts in the humification index (HIX) and the biological activity**
571 **index (BIX) during the 24-h incubation. Asterisks indicate significant differences identified by linear**
572 **regression analysis between initial and final treatments ($p<0.05$).**

573

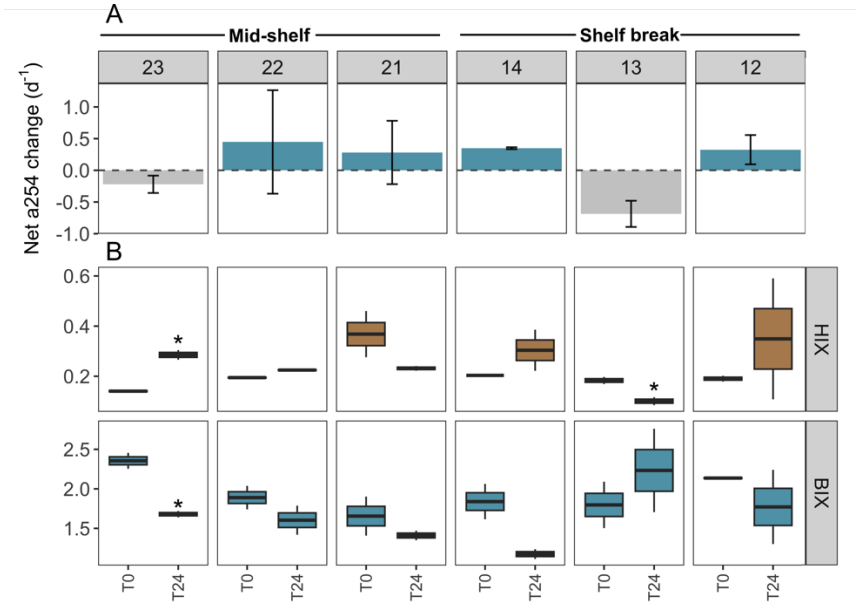

574

Figure 7. DOM transformations in the experimental setting without protists (pre-filtered by 0.7 µm) across stations in the mid-shelf and the shelf break front. A. Net changes in the absorbance at 254 nm (a254) from the chromophoric fraction of DOM ~~production as depicted by the absorbance intensity at 254 nm~~, a proxy of total DOM concentration. Dashed line indicates the limit between negative (i.e., consumption) ~~net DOM consumption (negative values)~~ and positive net a254 changes (i.e., accumulation) during the incubation period~~net DOM accumulation (positive values)~~. B. Shift in the humification index (HIX) and the biological activity index (BIX) during the 24-h incubation. Asterisks indicate significant differences identified by linear regression analysis between initial and final treatments (p<0.05).

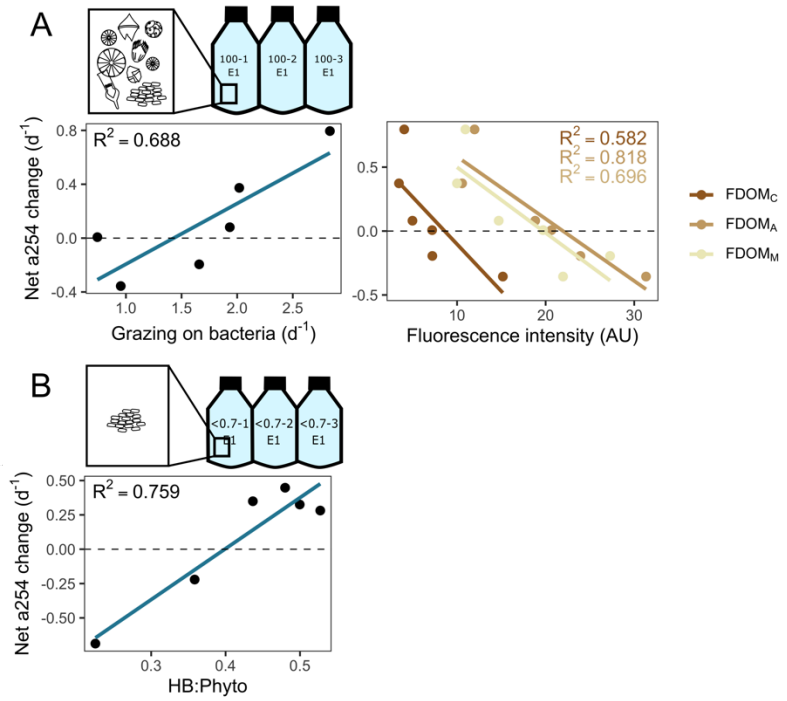

Figure 8. Main predictors of the net changes in the absorbance at 254 nm (a254) from the chromophoric fraction of DOM ~~dissolved organic matter (DOM) production~~ during incubations. A. Experimental setting with protists. Linear regression plots depict the relationship between net a254 changes ~~DOM production~~ and grazing on bacteria, and humic-like substances (as depicted by fluorophores $FDOM_C$, $FDOM_A$, and $FDOM_M$). B. Experimental setting without protists. Linear regression plot depicts the relationship between net ~~DOM production~~a245 changes and the ratio between heterotrophic bacteria (HB) and phytoplankton (Phyto) biomass. Dashed lines indicate the limit between negative (i.e., consumption) and positive (i.e., accumulation) net a254 changes~~net DOM consumption (negative values) and net DOM accumulation (positive values)~~.

4 Discussion

4.1 Microbial food web structure

Plankton composition and distribution varied notably across blooming and non-blooming stations, with station 14 standing out for its atypical plankton structure within a bloom region. Dominated by a nanoplanktonic diatom and a small grazer community, this station also showed high bacterial biomass, likely due to low PO_4^{3-} and Si concentrations, but high DOC levels. Nanoplankton, particularly diatoms, cryptophytes, and haptophytes, were predominant across sampling stations, with cyanobacteria assumed to play a significant role in carbon fixation. Similar findings were reported in previous studies by Silva et al. (2009) and Negri et al. (2013~~;~~ 2016)~~Silva et al. (2009)~~, indicating the widespread dominance of plankton <5 µm in the region.

In the shelf break front, dinoflagellates dominated both photosynthetic and heterotrophic biomass, while ciliates were more abundant in the mid-shelf. Besides these spatial differences, the lack of a clear distribution pattern of plankton highlights the impact of mesoscale structures on spatial plankton heterogeneity (Lehahn et al., 2018), a feature proper of the Patagonian Shelf (Saraceno et al., 2024). Heterotrophic bacterial abundance was comparable to coastal summer values reported by Hozbor et al. (2013), Negri et al. (2016), and Garzón-Cardona et al. (2021). It exhibited a positive correlation with chlorophyll-a, but was negatively affected by HNP grazing. This dynamic suggests that bacterial populations are primarily regulated by grazing pressure and the availability of phytoplankton-derived DOM, rather than by nutrient limitation during periods of high productivity.

~~The composition and distribution of the plankton community varied notably between blooming and non-blooming stations across our study area. Station 14 separated from this ordination due to its unique plankton structure resembling non-blooming areas, despite its location within a blooming region. This anomaly may be attributed to the dominance of a single nanoplanktonic diatom species, which accounted for a significant portion of the photosynthetic biomass, alongside a predominantly ultra- and nano-sized protistan grazer community. Moreover, station 14 exhibited the highest bacterial biomass, suggesting a prevalence of small planktonic organisms favored by resource stoichiometry characterized by low PO_4^{3-} and Si concentrations but high surface DOC. Furthermore, the location of station 14, coastward of the 100 m isobath and outside the Malvinas Current jets, indicates that nutrient-rich upwelling events at this site may be intermittent (Franco et al., 2008.~~

~~The analysis of biomass distribution among photosynthetic plankton revealed the predominance of ultra- and nanophytoplankton, with solitary diatoms, cryptophytes, haptophytes, and *Azadinium* like dinoflagellates being the most notable representatives within these size classes. Similar findings were reported in previous studies by Negri et al. (2013, 2016) and Silva et al. (2009), indicating the widespread dominance of ultraphytoplankton, primarily *Synechococcus*, in the region. Although cyanobacteria were not quantified in our study, they are assumed to play a crucial role in carbon fixation and immobilization, particularly during warm months. In the shelf break area, nano-sized phytoplankton, particularly diatoms, were dominant, as reported by Carreto et al. (2016). Micro-sized phytoplankton biomass was mostly comprised of photosynthetic dinoflagellates, followed closely by diatoms, consistent with findings by Ferronato et al. (2021, 2023), in the mid-shelf and shelf break areas during spring conditions.~~

~~Dinoflagellates also dominated the biomass of phagotrophic protists, with *Noctiluca scintillans* and nano-sized dinoflagellates being the primary contributors, as observed by (Carreto et al., 2016) in the shelf break area.~~

~~Ciliates, particularly nano-sized taxa, were the second most important contributors to heterotrophic biomass, followed by micro-sized ciliates such as *Laboea strobila*. No clear distribution patterns in protistan grazers were observed, a phenomenon well documented in marine habitats associated with factors such as compositional turnover, dispersal ability, differential environmental response, and interspecific interactions, coupled with local bloom timing (Grattepanche et al., 2016; Péquin et al., 2022; Snyder et al., 2021; Zhao et al., 2022). Mesoscale and submesoscale structures in the Patagonian Shelf create spatial heterogeneity, impacting the distribution of dissolved resources (Garzón Cardona et al., 2021) and chlorophyll a (Becker et al., 2023; Saraceno et al., 2024). The stirring produced by these processes, while understudied at the local scale, is fundamental in driving the three-dimensional distribution of plankton (Lehahn et al., 2018). Furthermore, the mosaic distribution of nutrients in turbulent areas may alter bacterial composition, with different nutrient affinities potentially reshaping the entire microbial interactome (Delgadillo-Nuño et al., 2024).~~

~~The abundance and biomass of heterotrophic bacteria fell within the reported minimum values for spring and summer in the study area, particularly resembling values typically observed during summer in the coastal zone (<50 m depth) (Garzón-Cardona et al., 2021; Hozbor et al., 2013; Negri et al., 2016). While prior studies in this sector did not establish a clear link between heterotrophic bacterial abundance and chlorophyll a, it is commonly noted that bacteria thrive in frontal regions with high phytoplankton concentrations and secondary production. In addition, previous research has indicated a positive correlation between bacterial abundance and dissolved organic carbon (Garzón-Cardona et al., 2021). In our study, we did not observe significant relationships between bacteria and DOM proxies (i.e., a254), while we did find a significant positive relationship with chlorophyll a. In turn, bacterial abundance exhibited a negative response to high HNP grazing pressure. This suggests that during periods of high productivity in spring, bacterial distribution is influenced not only by the supply of fresh DOM from phytoplankton but also by grazing-induced mortality. The intermittent coupling between bacteria and phytoplankton and the lack of reported relationships between bacteria and inorganic nutrients also suggest that bacteria are weakly resource-controlled in this area. Instead, considering that the control of grazing on bacterial biomass is more pronounced under conditions of low bottom-up regulation (Morán et al., 2017), our results suggest that under the examined conditions bacteria are top-down controlled, with maximum attainable biomass limited by grazing pressure as well as other unidentified sources of mortality.~~

4.2 Microbial trophic pathways

In oligotrophic areas, microbial food webs involve multi-step carbon transfer dominated by small organisms that efficiently recycle nutrients. By contrast, productive regions have shorter, more efficient food webs where carbon moves directly to higher trophic levels (Armengol et al., 2019). Our observations showed strong microbial trophic coupling across the mid-shelf and the shelf break front, however under more productive conditions, a fraction of primary producers escaped grazing. Mid-shelf stations, including post-bloom station 12, exhibited an "inverted pyramid" biomass structure, where consumer biomass exceeded that of their prey suggesting high trophic efficiency, as shown in former studies (McCauley et al., 2018). In the shelf break front, despite evidence of protistan herbivory, much of the phytoplankton biomass remained ungrazed likely due to strong top-down pressure from microcrustaceans on both phytoplankton and protistan grazers. This created a

more typical bottom-heavy biomass structure, indicative of high primary productivity where some primary production bypasses protist predation and is consumed by microcrustaceans or exported. Such a food web configuration achieves the highest carbon biomass, regardless of community composition (Kang et al., 2023). These observations align with previous findings in the shelf region, showing strong trophic coupling and minimal sinking of unused biomass, dominated by small phytoplankton (<5 µm) and balanced biomass levels of micro- and mesozooplankton (Negri et al., 2013).

~~Our findings are in line with previous observations in the region, emphasizing the tight trophic coupling and minimal sinking of unused prey biomass (Negri et al., 2013). This is attributed to the spatial uniformity of the trophic network composition, characterized by the dominance of small phytoplankton (<5 µm) and micro- and mesozooplankton groups, which exhibit comparable biomass magnitudes. Indeed, group-specific biomass distribution of <200 µm plankton in this study, revealed that except for station 13 and 14 that were at the bloom peak, mid shelf stations and station 12 (post bloom) showed a top heavy biomass distribution or inverted pyramid. Drivers of top heaviness are linked to high trophic transfer efficiency, faster turnover of prey than consumers, or omnivory that bypasses inefficient trophic levels (McCauley et al., 2018). Since the turnover of phytoplankton and bacteria is similar to that of protistan grazers, the most likely reason for the inverted pyramid structure is a high trophic efficiency and the presence of omnivore consumers. Protists are known to be highly efficient feeders (Weisse et al., 2016), particularly under high prey abundance, and trophic transfer is significantly increased by the presence of mixotrophs (Ward and Follows, 2016). Although mixotrophy was not directly assessed in this study, the predominance of nanoflagellates among protistan grazers implies a potential significant role of mixotrophy in shaping the trophic structure of the microbial community (Edwards, 2019). In contrast, the classical bottom heavy pyramid biomass structure of plankton was registered under bloom peak at shelf break stations 13 and 14. Despite intense predation on phytoplankton in the shelf break stations, the biomass accumulation resulting from a higher carrying capacity, driven by local upwelling, was sufficient to maintain the typical biomass pyramid structure, with photosynthetic taxa dominating plankton biomass. This type of food web structure attains the highest carbon biomass regardless of community composition (Kang et al., 2023), and suggests that under productive conditions within the upwelling front, a fraction of primary production escapes predation by protists and is either exploited by microcrustaceans or advected by mixing or sinking processes.~~

Our findings showed active growth of heterotrophic bacteria across all stations, while phytoplankton exhibited low net growth or biomass yield, except at two stations undergoing developing bloom stages (14 and 21). Heterotrophic bacteria, despite having half the biomass of phytoplankton, was selectively preyed by protistan grazers, accounting for 72% of bacterial production in mid-shelf stations and 83% in the shelf break front (Fig. 9). This preference for bacteria likely stems from their higher growth rate compared to phytoplankton, as protistan grazing is primarily triggered by prey growth rate rather than biomass (Banse, 1982; Calbet and Landry, 2004; Chen et al., 2009). Regarding the low phytoplankton growth rates observed in this study, an additional factor beyond bloom timing may involve UV photoinhibition, which can affect some eukaryotic pigmented plankton when exposed to deck conditions. Although light conditions were carefully controlled during handling and the incubator was covered with a special net to prevent overexposure, continuous light

exposure cannot fully replicate the natural mitigation of UV stress provided by vertical mixing in the water column (Häder et al., 2015). Laws et al. (2000) noted unrealistic growth estimates, attributing the negative effects of UV exposure to phytoplankton incubation at the surface. Simulating natural UV exposure remains a common challenge in most incubation experiments, where communities experience more stable light conditions.~~Our results denoted active growth of heterotrophic bacteria in all stations, while phytoplankton evidenced low net growth or biomass yield. Low growth rate of phytoplankton was only detected in station 21 at the bloom initiation and in station 14 at the last stage of the ascending bloom ramp. Despite possessing half the biomass of phytoplankton, grazers selectively preyed upon heterotrophic bacteria and accounted for 72% of bacterial production in the mid-shelf stations while phytoplankton production was not significantly affected by grazing. This selective grazing on bacteria can likely be attributed to their higher growth rate compared to that of phytoplankton, as protistan grazing is known to be activated in response to changes in prey availability (Banse, 1982; Calbet and Landry 2004; Chen et al., 2009). In fact, grazing by HNP showed a negative relationship with bacterial biomass, denoting that prey growth is a better activator than their biomass.~~

~~Consequently,~~Our results showed that bacteria exhibited growth advantages over phytoplankton across the examined environmental gradient but were concurrently more vulnerable to grazing pressure. This compensatory grazing on fast-growing bacteria has been previously observed in productive environments such as the California Current (Goericke, 2011; Taylor and Landry, 2018; Landry et al., 2023~~; Taylor and Landry, 2018~~), as well as in the oligotrophic Warm Taiwan Current (Chiang et al., 2014). The suggested mechanism underlying this trophic interaction posits that increased phytoplankton-DOM production fosters the growth of resource-efficient bacteria, as suggested by the tight coupling between bacteria and phytoplankton biomass. However, the heightened growth, coupled with a diminished allocation of energy to defensive skills, renders these bacteria susceptible to selective grazing (Taylor and Landry, 2018).

The situation in the more productive shelf break ~~area~~front~~,~~ shifted toward a coupled predation upon both prokaryotes and phytoplankton (Fig. 9~~a~~). Grazing accounted for 83% of bacterial production and 154% of phytoplankton production. Despite limited growth, phytoplankton faced substantial grazing pressure, possibly facilitated by shared predators with bacteria. This trophic interaction aligns with the enhanced microbial loop hypothesis (Taylor and Landry, 2018~~b~~), suggesting that small phytoplankton is increasingly grazed as a byproduct of grazers actively preying on bacteria under conditions of rising productivity. Under this scenario, grazing on picophytoplankton is density-independent and occurs due to the presence of shared common grazers with bacteria. ~~Across stations, density-dependent control mechanisms further regulated the standing stock of bacteria, with mechanisms reducing population density likely conferring benefits by preventing rapid resource depletion.~~ Overall, bacteria appeared to be positively regulated by commensalism with phytoplankton and negatively by grazing, constituting a primary carbon source for protistan grazers regardless of the productivity level.

An additional factor contributing to grazing selectivity across productivity areas may be related to grazer community composition, which differed between the mid-shelf and the shelf break front, with ciliates more concentrated on the mid-shelf and heterotrophic dinoflagellates more associated with shelf break stations (especially in stations 12 and 13). In contrast, phytoplankton structure showed no distinct regional differences.

Ciliates primarily select prey based on size due to their oral diameter, while dinoflagellates employ diverse feeding strategies, allowing them access to a broader range of prey sizes. This trait positions dinoflagellates as key grazers in meso- and eutrophic environments, such as upwelling areas (e.g., Hansen et al., 1997; Sherr and Sherr, 2007; Calbet, 2008), enabling them to effectively target both bacteria and larger phytoplankton.

4.3 Short-term DOM pathways

~~A general trend denoting weak DOM limitation of bacterial growth was found, as even in the experiments without DOM-producing phytoplankton, organic matter accumulated in most experiments.~~ Throughout the experiments, substantial bacterial proliferation and minimal or no phytoplankton growth were observed to occur alongside the active biodegradation of organic matter, as evidenced by a decrease in the biological index (BIX) and an increase in the humification index (HIX)~~During the experiments, high bacterial growth, and net zero or low phytoplankton growth coincided with active biodegradation of organic matter, as indicated by the decline in the biological index (BIX) and the rise in the humification index (HIX)~~. The general decreasing trend of BIX during the incubation and its similar behaviour in the absence of protist confirms a bacterial effect and suggests that bacteria are rapidly consuming recently produced phytoplankton exudates. Comparable observations have shown that bacteria produce humic-like substances from protistan plankton precursors in controlled environments absent of terrestrial influence (Gruber et al., 2006; Romera-Castillo et al., 2011; Lechtenfeld et al., 2015; Kinsey et al., 2018; Osburn et al., 2019), underscoring the pivotal role of microbial communities in converting DOM into refractory substances over brief timescales~~Similar observations have shown bacterial production of humic-like substances from protistan plankton precursors under experimental conditions devoid of terrestrial influence (Gruber et al., 2006; Kinsey et al., 2018; Lechtenfeld et al., 2015; Osburn et al., 2019; Romera-Castillo et al., 2011), underscoring the significance of microbial communities in immobilizing DOM in the form of refractory substances over short timescales~~. The described carbon route partially explains why the region acts as a carbon sink throughout most of the year (Kahl et al., 2017), irrespective of the magnitude of ~~the~~ primary productivity ~~magnitude~~, and emphasize the critical role of the microbial carbon pump (Jiao et al., 2010) as a key carbon sequestration pathway ~~in~~ on the northern Patagonian Shelf. While these findings highlight its importance, the seasonal relevance of this mechanism remains to be explored.

The accumulation of a fraction of DOM, as indicated by a254, was not limited to stations experiencing active phytoplankton growth, indicating that net DOM release is not necessarily tied to specific phenological stages, as previously suggested (Bachi et al., 2023). Moreover, accumulation occurred under diverse phytoplankton assemblages~~it was not correlated with phytoplankton species composition~~, implying a low level of specialization in the bacterial utilization of species-specific DOM substances, a trait that becomes apparent under conditions of high resource availability (Sarmento et al., 2016).

The complexity of DOM, reflected by the prevalence of humic-like compounds ($FDOM_C$, $FDOM_A$, and $FDOM_M$), emerged as a key factor influencing its bacterial utilization. A net consumption of the DOM fraction, as estimated by a254, was observed when the initial pool contained a significant proportion of low-reactivity compounds, influenced by the phenological status of the sampling site, as indicated by satellite chlorophyll-a

trends. At stations 23 and 21, low prior chlorophyll-a indicated limited recent autochthonous DOM production. However, bacterial activity differed between the two stations. At station 23, elevated bacterial activity resulted in a notable increase in DOM complexity and net consumption under both treatments, indicating that bacteria depended on a substantial initial labile DOM pool ($FDOM_T$), despite the predominance of refractory compounds. In contrast, station 21 exhibited low bacterial activity, with the a254 DOM fraction shifting from consumption to accumulation in the absence of protists. This indicated bacterial reliance on phytoplankton DOM exudates when the DOM pool is primarily refractory.

At station 13, the opposite pattern was observed, with the a254 DOM fraction shifting from weak accumulation in the presence of protists, to consumption in the absence of protists. Here, a higher proportion of labile DOM facilitated bacterial activity. Low phytoplankton-to-bacteria biomass ratios indicated that bacterial DOM consumption was masked by phytoplankton biomass but became evident without protists. However, DOM accumulation may also reflect viral lysis, as suggested by HIX decreases and BIX increases, alongside low bacterial growth and grazing. ~~Instead, the degree of complexity of DOM expressed as the prevalence of humic compounds ($FDOM_C$, $FDOM_A$, and $FDOM_M$), emerged as a primary factor determining its utilization by bacteria. Detectable consumption occurred when the initial DOM pool presented a high contribution of low reactivity compounds, likely resulting from the phenological status of the sampling point as depicted by the temporal progression of satellite chlorophyll-a. This scenario was observed at stations 23 and 21, where sampling was preceded by low chlorophyll-a content, indicating limited autochthonous production of fresh DOM in the preceding month. However, the differences in bacterial growth and FDOM inferred biodegradation at both stations suggest variations in bacterial activity. At station 23, intense bacterial activity was evidenced by the significant increase in the complexity of DOM and the net DOM consumption under both treatments. Despite the high contribution of refractory compounds in this site ($FDOM_C$, $FDOM_A$, and $FDOM_M$), the initial labile DOM pool was also high (particularly $FDOM_T$), denoting that bacteria may have sustained their growth upon this labile initial stock over the 24 h incubation under the absence of DOM-producing phytoplankton. Interestingly, under the absence of protists, DOM consumption shifted to accumulation in station 21. At this station, a notable abundance of initial refractory compounds was observed. In contrast to observations at station 23, bacterial activity was low, as indicated by a low growth rate and no detectable biodegradation of DOM. Therefore, the apparent decrease of bacterial DOM utilization under the absence of protists, suggests that bacterial reliance on phytoplankton DOM exudates increases when the existing DOM pool consists primarily of refractory compounds. Despite similar phenological stage, this situation was not observed in station 22, where the degree on refractory compound was lower. This suggests the presence of other sources of labile DOM that may not be adequately represented by total chlorophyll-a measurements, such as *Synechococcus*, a significant picophytoplankton genus in the shelf area (Silva et al., 2009) known to contribute to bioavailable DOM production (Zheng et al., 2019).~~

~~The opposite scenario, i.e., a shift from weak DOM accumulation to DOM consumption under the absence of protists, was observed in station 13. Here, the initial proportion of labile DOM was higher, denoting that DOM bioavailability did not restrict bacterial activity. This station displayed the lowest biomass ratio between phytoplankton and bacteria, indicating that DOM consumption in the absence of protists occurred when the~~

~~initial phytoplankton biomass significantly surpassed that of heterotrophic bacteria. This suggests that the initial phytoplankton biomass masked intense bacterial DOM utilization, which only became evident upon the removal of protists. However, DOM accumulation might be overestimated due to the input of DOM lysates resulting from viral lysis. Indeed, the decrease in HIX alongside the increase in BIX observed in station 13 under both treatments suggests that viruses are transferring bacterial biomass into the labile DOM pool (Proctor and Fuhrman, 1991). The low bacterial growth and grazing at this site along with the station's bloom timing further support this notion, as it suggests that sampling occurred at the transition between grazing control to viral control of bacterial biomass. Indeed, the latter tends to occur under low grazing pressure (Bettarel et al., 2004; Pasulka et al., 2015).~~ Overall, ~~the fact that DOM accumulation occurred even in the absence of protists, indicates that bacteria are the main source of DOM as previously noted (Gruber et al., 2006).~~ t~~T~~he initial proportion of refractory compounds better predicted the net DOM production by providing insights on microbial succession trajectories.

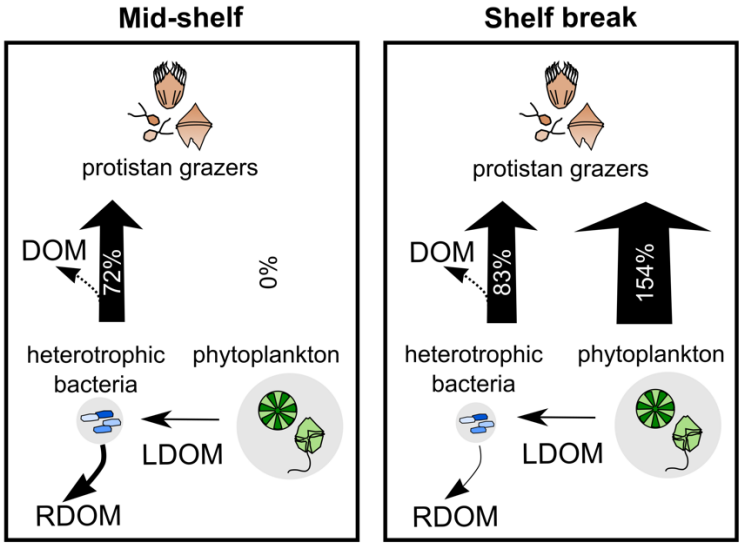

Figure 9. ~~**Grazing mediated**~~**Schematic representation of DOM pathways** ~~**of DOM**~~ **during the productive season** ~~**in**~~ **on the Patagonian Shelf, contrasting the mid-shelf (low-to-moderate productivity, left panel) with the shelf break front (high productivity, right panel).** ~~**A.**~~ **Phytoplankton biomass (background circle size) was twice that of bacteria, with selective grazing on bacteria balancing their rapid growth across sampling areas. Grazing on phytoplankton increased under higher productivity, aligning with the enhanced microbial loop hypothesis. Heterotrophic bacteria were key in shaping DOM quality, utilizing labile DOM (LDOM) from phytoplankton and contributing to the storage of refractory DOM (RDOM), even without DOM-producing protists. RDOM production was more pronounced mid-shelf than at the shelf break. Bacterial grazing influenced the net production of the a254 DOM fraction, with intense grazing leading to DOM accumulation likely through reduced bacterial biomass and egested organic material. Arrow thickness represents grazing pressure, with percentages indicating daily grazed productivity.**

~~While phytoplankton biomass was found to be twice that of bacteria, a selective grazing on bacteria was observe compensating for their fast growth rate along the productivity gradient. In turn, grazing on phytoplankton increased with rising productivity, suggesting that phytoplankton, particularly smaller cells, are increasingly grazed as a byproduct of intense grazing on bacteria, aligning with the enhanced microbial loop hypothesis. Heterotrophic bacteria were the primary agents shaping DOM quality, capable of storing carbon in the refractory DOM pool (rDOM) even in the absence of DOM-producing protists. However, the production of rDOM was more conspicuous in mid-shelf stations than in the shelf break. B. Grazing on bacteria influenced the net production of DOM. Arrows thickness represents grazing pressure. Pronounced bacterial grazing led to an accumulation of DOM,likely by reducing the biomass of bacterial standing stock and by contributing with egestion organic substances.~~

The a254 DOM fraction also tended to accumulate under high bacterial mortality due to grazing. Our results evidenced a selective grazing on bacteria compensating for their fast growth rate~~that carbon was primarily channeled from prokaryotes to protistan grazers, bypassing slower growing phytoplankton~~. This group-specific grazing mortality aligns well with the grazing selectivity model, wherein grazers exhibit preferences against high-growth-rate organisms, establishing a tight coupling between growth advantages and grazing vulnerability across environmental gradients (Landry et al., 2023). Our experimental data not only support this hypothesis but also provide new insights into the repercussions of bacterial grazing on dissolved carbon stocks (Fig. 9~~b~~). Specifically, our results suggest that grazing on bacteria can lead to an accumulation of DOM produced by phytoplankton by reducing the biomass of bacterial standing stock. In addition, protistan grazing may contribute to the DOM pool by releasing bacterial carbon (Taylor et al., 1985). However, bacteria may not immediately utilize this DOM source, as adapting their enzymatic machinery to target new compounds requires additional energy expenditure, resulting in less efficient resource utilization (Baña et al., 2014). Similar results were observed in polar waters, where high protistan bacterivory was associated with DOM accumulation (Lund Paulsen et al., 2019). Our observations carry biogeochemical implications, as intense bacterial grazing implies that bacterial biomass becomes available to higher trophic levels, thereby circumventing the DOM cycle. In other words, while most bacterial biomass is directed by protistan grazers toward higher trophic levels, it also partially diverts the production of DOM lysates by viral lysis (Suttle, 2005). Our experimental results also indicate that intense grazing only partially compensates for this carbon route, as protistan grazing contributes with additional DOM substances while ~~as~~ a fraction of phytoplankton-derived DOM remains unexploited by bacteria over short timescales.

Protistan grazing is widely recognized as the primary driver of phytoplankton mortality (Calbet and Landry, 2004) and is an important mortality source for heterotrophic bacteria (Weinbauer and Peduzzi, 1995). However, viral lysis can achieve comparable mortality rates in both phytoplankton and bacterial populations to that caused by protistan grazers. Discerning the viral impact within incubation bottles can be challenging, as viral activity may not only contribute to cell lysis but has been observed to stimulate prey availability for protists, potentially through the release of cellular lysates or by reducing competition (Staniewski and Short, 2014). In our study, while protist grazing was considered the primary cause of bacterial and phytoplankton mortality, we

acknowledge that viral lysis may have also played an unrecognized but significant role in the dilution experiments.

The fate of grazing-derived DOM remains uncertain in our experimental setup, as it could either serve as a potential source for bacterial utilization, thus establishing ~~a~~ positive longer-term predator-prey feedback not captured in our 24-h experiment, or contribute to the complex DOM pool, feeding into the refractory fraction. Indeed, previous observations revealed that DOM derived from protistan grazers varies in its bioavailability (Taylor et al., 1985), and their complexity is further shaped by taxa composition (Nagata and Kirchman, 1992; Gruber et al., 2006~~; Nagata and Kirchman, 1992~~). In our experiments, we did not observe a clear trend in DOM transformation between treatments with and without protists, indicating that bacteria remain as the primar~~il~~y ~~shapers~~ drivers of DOM quality. Overall, our finding revealed that under high bacterial growth rate that follows the onset of the productive season, protistan grazers not only channels carbon through remineralization but also, foster the degree of DOM accumulation by reducing DOM-degrading bacterial stock and/or contributing with egestion substances. Additionally, instead of acting solely as a sink of carbon through mineralization of organic compounds, bacteria serve as a crucial link between assimilatory CO_2 and higher trophic levels.

Data availability

DOI: 10.5281/zenodo.11662261

Authors contribution

CLA conceptualized, designed, and carried out the experiments, analyzed plankton samples and acquired funding. JEGC, AM and ASG analyzed DOC, optical properties of DOM ~~CDOM, FDOM~~ and nutrients samples and interpreted the results. JEGC performed the PARAFAC multivariate algorithm and calculated fluorescence indices. RS analyzed plankton samples and performed biomass calculations. JCM contributed to the numerical methodology design and the conceptualization of overarching~~reaching~~ goals. LARE analyzed and interpreted CTD data and Moderate Resolution Imaging Spectroradiometer (MODIS) Aqua images of chlorophyll-a. RL coordinated responsibilities for the research activities planning and execution, acquired funding and contributed to the conceptualization of overarching~~reaching~~ goals. CLA prepared the manuscript with contributions from all co-authors.

Competing interests

The authors declare no competing interests.

Acknowledgments

We are thankful to the crew of the RV "Dr. Bernardo Houssay" of Prefectura Naval Argentina for their support on field activities and sampling. This study was supported by the National Agency for Promotion of Science and Technology (FONCYT-PICT 0467–2010 and FONCYT-PICT 2386-2017), the National Scientific and Technical Research Council (CONICET-PIP 11220200102681CO) and by the Argentine Oceanographic

Institute (IADO, CONICET-UNS). The authors acknowledge that language checking and spelling improvements were done by ChatGPT (powered by OpenAI's language model, GPT-3; http://openai.com).

References

~~Azam, F., Fenchel, T., Field, J., Gray, J., Meyer Reil, L., and Thingstad, F.: The Ecological Role of Water-Column Microbes in the Sea, Mar Ecol Prog Ser, 10, 257–263, https://doi.org/10.3354/meps010257, 1983.~~

Armengol, L., Calbet, A., Franchy, G., Rodríguez-Santos, A., and Hernández-León, S.: Planktonic food web structure and trophic transfer efficiency along a productivity gradient in the tropical and subtropical Atlantic Ocean. Sci Rep, 9, 2044, https://doi.org/10.1038/s41598-019-38507-9, 2019.

Bachi, G., Morelli, E., Gonnelli, M., Balestra, C., Casotti, R., Evangelista, V., Repeta, D. J., and Santinelli, C.: Fluorescent properties of marine phytoplankton exudates and lability to marine heterotrophic prokaryotes degradation, Limnol Oceanogr, 68, https://doi.org/10.1002/lno.12325, 2023.

Bai, Y., Su, R., Han, X., Zhang, C., and Shi, X.: Investigation of seasonal variability of CDOM fluorescence in the southern changjiang river estuary by EEM-PARAFAC, Acta Oceanologica Sinica, 34, 1–12, https://doi.org/10.1007/s13131-015-0714-8, 2015.

Baltar, F., Palovaara, J., Unrein, F., Catala, P., Horňák, K., Šimek, K., Vaqué, D., Massana, R., Gasol, J. M., and Pinhassi, J.: Marine bacterial community structure resilience to changes in protist predation under phytoplankton bloom conditions, ISME J, 10, 568–581, https://doi.org/10.1038/ismej.2015.135, 2016.

Baña, Z., Ayo, B., Marrasé, C., Gasol, J. M., and Iriberri, J.: Changes in bacterial metabolism as a response to dissolved organic matter modification during protozoan grazing in coastal Cantabrian and Mediterranean waters, Environ Microbiol, 16, 498–511, https://doi.org/10.1111/1462-2920.12274, 2014.

Banse, K.: Cell volumes, maximal growth rates of unicellular algae and ciliates, and the role of ciliates in the marine pelagial~~1,2~~, Limnol Oceanogr, 27, 1059–1071, https://doi.org/10.4319/lo.1982.27.6.1059, 1982.

~~Becker, F., Romero, S. I., and Pisoni, J. P.: Detection and characterization of submesoscale eddies from optical images: a case study in the Argentine continental shelf, Int J Remote Sens, 44, 3146–3159, https://doi.org/10.1080/01431161.2023.2216853, 2023.~~

Berden, G., Charo, M., Möller, O. O., and Piola, A. R.: Circulation and Hydrography in the Western South Atlantic Shelf and Export to the Deep Adjacent Ocean: 30°S to 40°S, J Geophys Res Oceans, 125, https://doi.org/10.1029/2020JC016500, 2020.

Berglund, J., Müren, U., Båmstedt, U., and Andersson, A.: Efficiency of a phytoplankton-based and a bacterial-based food web in a pelagic marine system, Limnol Oceanogr, 52, 121–131, https://doi.org/10.4319/lo.2007.52.1.0121, 2007.

~~Bettarel, Y., Sime-Ngando, T., Amblard, C., and Dolan, J.: Viral Activity in Two Contrasting Lake Ecosystems, Appl Environ Microbiol, 70, 2941–2951, https://doi.org/10.1128/AEM.70.5.2941-2951.2004, 2004.~~

Brandstetter, A., Sletten, R. S., Mentler, A., and Wenzel, W. W.: Estimating dissolved organic carbon in natural waters by UV absorbance (254 nm), Zeitschrift für Pflanzenernährung und Bodenkunde, 159, 605–607, https://doi.org/10.1002/jpln.1996.3581590612, 1996.

~~Brussaard, C. P. D.: Viral Control of Phytoplankton Populations – a Review, Journal of Eukaryotic Microbiology, 51, 125–138, https://doi.org/10.1111/j.1550-7408.2004.tb00537.x, 2004.~~

Calbet, A.: The trophic roles of microzooplankton in marine systems. ICES J, 65, 325-331, https://doi.org/10.1093/icesjms/fsn013, 2008.

Calbet, A. and Landry, M. R.: Phytoplankton growth-, microzooplankton grazing-, and carbon cycling in marine systems, Limnol Oceanogr Methods, 49, 51–57, https://doi.org/10.4319/lo.2004.49.1.0051, 2004.

Calbet, A. and Saiz, E.: How much is enough for nutrients in microzooplankton dilution grazing experiments?, J Plankton Res, 40, 109–117, https://doi.org/10.1093/plankt/fbx070, 2018.

~~Carreto, J. I., Montoya, N. G., Carignan, M. O., Akselman, R., Acha, E. M., and Derisio, C.: Environmental and biological factors controlling the spring phytoplankton bloom at the Patagonian shelf-break front – Degraded fucoxanthin pigments and the importance of microzooplankton grazing, Prog Oceanogr, 146, 1–21, https://doi.org/10.1016/j.pocean.2016.05.002, 2016.~~

~~Cavicchioli, R., Ripple, W. J., Timmis, K. N., Azam, F., Bakken, L. R., Baylis, M., Behrenfeld, M. J., Boetius, A., Boyd, P. W., Classen, A. T., Crowther, T. W., Danovaro, R., Foreman, C. M., Huisman, J., Hutchins, D. A., Jansson, J. K., Karl, D. M., Koskella, B., Mark Welch, D. B., Martiny, J. B. H., Moran, M. A., Orphan, V. J., Reay, D. S., Remais, J. V., Rich, V. I., Singh, B. K., Stein, L. Y., Stewart, F. J., Sullivan, M. B., van Oppen, M. J. H., Weaver, S. C., Webb, E. A., and Webster, N. S.: Scientists' warning to humanity: microorganisms and climate change, Nat Rev Microbiol, 17, 569–586, https://doi.org/10.1038/s41579-019-0222-5, 2019.~~

Chen, B., Liu, H., Landry, M. R., DaI, M., Huang, B., and Sune, J.: Close coupling between phytoplankton growth and microzooplankton grazing in the western South China Sea, Limnol Oceanogr, 54, 1084–1097, https://doi.org/10.4319/lo.2009.54.4.1084, 2009.

Chiang, K.-P., Tsai, A.-Y., Tsai, P.-J., Gong, G.-C., Huang, B.-Q., and Tsai, S.-F.: The influence of nanoflagellates on the spatial variety of picoplankton and the carbon flow of the microbial food web in the oligotrophic subtropical pelagic continental shelf ecosystem, Cont Shelf Res, 80, 57–66, https://doi.org/10.1016/j.csr.2014.02.019, 2014.

Coble, P. G.: Characterization of marine and terrestrial DOM in seawater using excitation-emission matrix spectroscopy, Mar Chem, 51, 325–346, https://doi.org/10.1016/0304-4203(95)00062-3, 1996.

~~Delgadillo-Nuño, E., Teira, E., Pontiller, B., Lundin, D., Joglar, V., Pedrós-Alió, C., Fernández, E., Pinhassi, J., and Martínez-García, S.: Coastal upwelling systems as dynamic mosaics of bacterioplankton functional specialization, Front Mar Sci, 10, https://doi.org/10.3389/fmars.2023.1259783, 2024.~~

Delgado, A. L., Hernández-Carrasco, I., Combes, V., Font-Muñoz, J., Pratolongo, P. D., and Basterretxea, G.: Patterns and Trends in Chlorophyll-a Concentration and Phytoplankton Phenology in the Biogeographical Regions of Southwestern Atlantic, J Geophys Res Oceans, 128, https://doi.org/10.1029/2023JC019865, 2023.

Drozdova, A. N., Krylov, I. N., Nedospasov, A. A., Arashkevich, E. G., and Labutin, T. A.: Fluorescent signatures of autochthonous dissolved organic matter production in Siberian shelf seas. Front Mar Sci 9:872557. https://doi:10.3389/fmars.2022.872557, 2022.

Edwards, K. F.: Mixotrophy in nanoflagellates across environmental gradients in the ocean, Proceedings of the National Academy of Sciences, 116, 6211–6220, https://doi.org/10.1073/pnas.1814860116, 2019.

Ferronato, C., Guinder, V. A., Chidichimo, M. P., López Abbate, C., and Amodeo, M.: Zonation of protistan plankton in a productive area of the Patagonian shelf: Potential implications for the anchovy distribution, Food Webs, 29, e00211, https://doi.org/10.1016/j.fooweb.2021.e00211, 2021.

Ferronato, C., Berden, G., Rivarossa, M., and Guinder, V. A.: Wind-driven currents and water masses shape spring phytoplankton distribution and composition in hydrologically complex, productive shelf waters, Limnol Oceanogr, 68, 2195–2210, https://doi.org/10.1002/lno.12413, 2023.

Franco, B. C., Piola, A. R., Rivas, A. L., Baldoni, A., and Pisoni, J. P.: Multiple thermal fronts near the Patagonian shelf break, Geophys Res Lett, 35, https://doi.org/10.1029/2007GL032066, 2008.

Franco, B. C., Palma, E. D., Combes, V., Acha, E. M., and Saraceno, M.: Modeling the Offshore Export of Subantarctic Shelf Waters From the Patagonian Shelf, J Geophys Res Oceans, 123, 4491–4502, https://doi.org/10.1029/2018JC013824, 2018.

Garzón-Cardona, J. E., Guinder, V. A., Alonso, C., Martínez, A. M., Pantoja-Gutiérrez, S., Kopprio, G. A., Krock, B., and Lara, R. J.: Chemically unidentified dissolved organic carbon: A pivotal piece for microbial activity in a productive area of the Northern Patagonian shelf, Mar Environ Res, 167, 105286, https://doi.org/10.1016/j.marenvres.2021.105286, 2021.

Goericke, R.: The structure of marine phytoplankton communities-patterns, rules and mechanisms, California Cooperative Oceanic Fisheries Investigation Reports, 52, 182–197, 2011.

Grattepanche, J. D., McManus, G. B., and Katz, L. A.: Patchiness of Ciliate Communities Sampled at Varying Spatial Scales along the New England Shelf, PLoS One, 11, e0167659, https://doi.org/10.1371/journal.pone.0167659, 2016.

Gruber, D. F., Simjouw, J.-P., Seitzinger, S. P., and Taghon, G. L.: Dynamics and characterization of refractory dissolved organic matter produced by a pure bacterial culture in an experimental predator-prey system, Appl Environ Microbiol, 72, 4184–4191, https://doi.org/10.1128/AEM.02882-05, 2006.

Hach, P. F., Marchant, H. K., Krupke, A., Riedel, T., Meier, D. V., Lavik, G., Holtappels, M., Dittmar, T., and Kuypers, M. M. M.: Rapid microbial diversification of dissolved organic matter in oceanic surface waters leads to carbon sequestration, Sci Rep, 10, 13025, https://doi.org/10.1038/s41598-020-69930-y, 2020.

Häder, D. P., Williamson, C. E., Wängberg, S. Å., Rautio, M., Rose, K. C., Gao, K., Helbling, W. E., Sinha, R. P., and Worrest, R.: Effects of UV radiation on aquatic ecosystems and interactions with other environmental factors. Photochem Photobiol Sci, 14(1), 108-126, https://doi:10.1039/c4pp90035a, 2015.

Hansen, P. J., Bjørnsen, P. K., and Hansen, B. W.: Zooplankton grazing and growth: Scaling within the 2-2,000-µm body size range. Limnol Oceanogr, 42, 687-704, https://doi.org/10.4319/lo.1997.42.4.0687, 1997.

Hillebrand, H., Dürselen, C., Kirschtel, D., Pollingher, U., and Zohary, T.: Biovolume calculation for pelagic and benthic microalgae, J Phycol, 35, 403–424, https://doi.org/10.1046/j.1529-8817.1999.3520403.x, 1999.

Hozbor, M. C., Hernández, D. R., Cucchi Colleoni, A. D., Costagliola, M. C., and Peressutti, S. R.: Biomasa y distribución espacial del bacterioplancton en el sector norte de la plataforma continental argentina (34º S-41º S), Revista de Investigación y Desarrollo Pesquero, 23, 145–160, 2013.

Huguet, A., Vacher, L., Relexans, S., Saubusse, S., Froidefond, J. M., and Parlanti, E.: Properties of fluorescent dissolved organic matter in the Gironde Estuary, Org Geochem, 40, 706–719, https://doi.org/10.1016/j.orggeochem.2009.03.002, 2009.

Hutchins, D. A. and Fu, F.: Microorganisms and ocean global change, Nat Microbiol, 2, 17058, https://doi.org/10.1038/nmicrobiol.2017.58, 2017.

Irigoien, X., Flynn, K. J., and Harris, R. P.: Phytoplankton blooms: a 'loophole' in microzooplankton grazing impact?, J Plankton Res, 27, 313–321, https://doi.org/10.1093/plankt/fbi011, 2005.

Jeffrey, S. W. and Humphrey, G. F.: New spectrophotometric equations for determining chlorophylls a, b, c1 and c2 in higher plants, algae and natural phytoplankton, Biochemie und Physiologie der Pflanzen, 167, 191–194, https://doi.org/10.1016/S0015-3796(17)30778-3, 1975.

Jiao, N., Herndl, G. J., Hansell, D. A., Benner, R., Kattner, G., Wilhelm, S. W., Kirchman, D. L., Weinbauer, M. G., Luo, T., Chen, F., and Azam, F.: Microbial production of recalcitrant dissolved organic matter: long-term carbon storage in the global ocean. Nat Rev Microbiol, 8, 593–599, https://doi.org/10.1038/nrmicro2386, 2010.

~~Jiao, N., Luo, T., Chen, Q., Zhao, Z., Xiao, X., Liu, J., Jian, Z., Xie, S., Thomas, H., Herndl, G. J., Benner, R., Gonsior, M., Chen, F., Cai, W. J., and Robinson, C.: The microbial carbon pump and climate change, Nat Rev Microbiol, 22, 408–419, https://doi.org/10.1038/s41579-024-01018-0, 2024.~~

Jørgensen, L., Stedmon, C. A., Kragh, T., Markager, S., Middelboe, M., and Søndergaard, M.: Global trends in the fluorescence characteristics and distribution of marine dissolved organic matter. Mar Chem, 126(1–4), 139–148, https://doi.org/10.1016/j.marchem.2011.05.002, 2011.

Kahl, L. C., Bianchi, A. A., Osiroff, A. P., Pino, D. R., and Piola, A. R.: Distribution of sea-air CO2 fluxes in the Patagonian Sea: Seasonal, biological and thermal effects, Cont Shelf Res, 143, 18–28, https://doi.org/10.1016/j.csr.2017.05.011, 2017.

Kanayama, T., Kobari, T., Suzuki, K., Yoshie, N., Honma, T., Karu, F., and Kume, G.: Impact of microzooplankton grazing on the phytoplankton community in the Kuroshio of the East China sea: A major trophic pathway of the Kuroshio ecosystem, Deep-Sea Res I: Oceanogr Res Pap~~Deep Sea Research Part I: Oceanographic Research Papers~~, 163, 103337, https://doi.org/10.1016/j.dsr.2020.103337, 2020.

Kang, H. C., Jeong, H. J., Ok, J. H., Lim, A. S., Lee, K., You, J. H., Park, S. A., Eom, S. H., Lee, S. Y., Lee, K. H., Jang, S. H., Yoo, Y. Du, Lee, M. J., and Kim, K. Y.: Food web structure for high carbon retention in marine plankton communities, Sci Adv, 9, https://doi.org/10.1126/sciadv.adk0842, 2023.

Kattner, G. and Becker, H.: Nutrients and organic nitrogenous compounds in the marginal ice zone of the Fram Strait, J~~ournal of~~ Mar~~ine~~ Syst~~ems~~, 2, 385–394, https://doi.org/10.1016/0924-7963(91)90043-T, 1991.

Kinsey, J. D., Corradino, G., Ziervogel, K., Schnetzer, A., and Osburn, C. L.: Formation of c~~C~~hromophoric d~~D~~issolved o~~O~~rganic ~~Matter~~ matter by ~~Bacterial~~ bacterial ~~Degradation~~ degradation of ~~Phytoplankton~~phytoplankton-~~Derived~~ derived ~~Aggregates~~aggregates, Front Mar Sci, 4, https://doi.org/10.3389/fmars.2017.00430, 2018.

Kujawinski, E. B., Del Vecchio, R., Blough, N. V., Klein, G. C., and Marshall, A. G.: Probing molecular-level transformations of dissolved organic matter: insights on photochemical degradation and protozoan modification of DOM from electrospray ionization Fourier transform ion cyclotron resonance mass spectrometry, Mar Chem, 92, 23–37, https://doi.org/10.1016/j.marchem.2004.06.038, 2004.

Landry, M. R. and Hassett, R. P.: Estimating the grazing impact of marine micro-zooplankton, Mar Biol, 67, 283–288, https://doi.org/10.1007/BF00397668, 1982.

Landry, M. R., Stukel, M. R., Selph, K. E., and Goericke, R.: Coexisting picoplankton experience different relative grazing pressures across an ocean productivity gradient, Proc Natl Acad Sci USA~~Proceedings of the National Academy of Sciences~~, 120, https://doi.org/10.1073/pnas.2220771120, 2023.

Laruelle, G. G., Cai, W.-J., Hu, X., Gruber, N., Mackenzie, F. T., and Regnier, P.: Continental shelves as a variable but increasing global sink for atmospheric carbon dioxide, Nat Commun, 9, 454, https://doi.org/10.1038/s41467-017-02738-z, 2018.

Laws, E. A, Landry, M. R., Barber, R. T., Campbell, L., Dickson, M.-L., and Marra J.: Carbon cycling in primary production bottle incubations: Inferences from grazing experiments and photosynthetic studies using ^{14}C and ^{18}O in the Arabian Sea, Deep Sea Res Part II, 47, 1339-1352, https://doi.org/10.1016/S0967-0645(99)00146-0, 2000.

Lechtenfeld, O. J., Hertkorn, N., Shen, Y., Witt, M., and Benner, R.: Marine sequestration of carbon in bacterial metabolites, Nat Commun, 6, 6711, https://doi.org/10.1038/ncomms7711, 2015.

Lee, M.-H., Osburn, C. L., Shin, K.-H., and Hur, J.: New insight into the applicability of spectroscopic indices for dissolved organic matter (DOM) source discrimination in aquatic systems affected by biogeochemical processes, Water Res, 147, 164–176, https://doi.org/10.1016/j.watres.2018.09.048, 2018.

Lehahn, Y., d'Ovidio, F., and Koren, I.: A Satellite-Based Lagrangian View on Phytoplankton Dynamics, Ann Rev Mar Sci, 10, 99–119, https://doi.org/10.1146/annurev-marine-121916-063204, 2018.

Lønborg, C., Álvarez-Salgado, X. A., Davidson, K., Martínez-García, S., and Teira, E.: Assessing the microbial bioavailability and degradation rate constants of dissolved organic matter by fluorescence spectroscopy in the coastal upwelling system of the Ría de Vigo, Mar Chem, 119, 121–129, https://doi.org/10.1016/j.marchem.2010.02.001, 2010.

Lønborg, C., Yokokawa, T., Herndl, G. J., and Antón Álvarez-Salgado, X.: Production and degradation of fluorescent dissolved organic matter in surface waters of the eastern north Atlantic ocean, Deep Sea Res~~earch~~ Part I: Oceanog~~raphic~~ Res~~earch~~ Pap~~ers~~, 96, 28–37, https://doi.org/10.1016/j.dsr.2014.11.001, 2015.

Lucas, A. J., Guerrero, R. A., Mianzán, H. W., Acha, E. M., and Lasta, C. A.: Coastal oceanographic regimes of the Northern Argentine Continental Shelf (34–43°S), Estuar Coast Shelf Sci, 65, 405–420, https://doi.org/10.1016/j.ecss.2005.06.015, 2005.

Lund Paulsen, M., Müller, O., Larsen, A., Møller, E. F., Middelboe, M., Sejr, M. K., and Stedmon, C.: Biological transformation of Arctic dissolved organic matter in a NE Greenland fjord, Limnol Oceanogr, 64, 1014–1033, https://doi.org/10.1002/lno.11091, 2019.

McCauley, D. J., Gellner, G., Martinez, N. D., Williams, R. J., Sandin, S. A., Micheli, F., Mumby, P. J., and McCann, K. S.: On the prevalence and dynamics of inverted trophic pyramids and otherwise top-heavy communities, Ecol Lett, 21, 439–454, https://doi.org/10.1111/ele.12900, 2018.

McKnight, D. M., Boyer, E. W., Westerhoff, P. K., Doran, P. T., Kulbe, T., and Andersen, D. T.: Spectrofluorometric characterization of dissolved organic matter for indication of precursor organic material and aromaticity, Limnol Oceanogr, 46, 38–48, https://doi.org/10.4319/lo.2001.46.1.0038, 2001.

~~Morán, X. A. G., Gasol, J. M., Pernice, M. C., Mangot, J., Massana, R., Lara, E., Vaqué, D., and Duarte, C. M.: Temperature regulation of marine heterotrophic prokaryotes increases latitudinally as a breach between bottom-up and top-down controls, Glob Chang Biol, 23, 3956–3964, https://doi.org/10.1111/gcb.13730, 2017.~~

Moran, M. A., Ferrer-González, F. X., Fu, H., Nowinski, B., Olofsson, M., Powers, M. A., Schreier, J. E., Schroer, W. F., Smith, C. B. and Uchimiya, M.: The Ocean's labile DOC supply chain. Limnol Oceanogr, 67, 1007-1021, https://doi.org/10.1002/lno.12053, 2022.

Nagata, T. and Kirchman, D.: Release of macromolecular organic complexes by heterotrophic marine flagellates, Mar Ecol Prog Ser, 83, 233–240, https://doi.org/10.3354/meps083233, 1992.

Negri, R. M., Silva, R. I., Segura, V., and Cucchi Colleoni, A. D.: Estructura de la comunidad del fitoplancton en el área de El Rincón, Mar Argentino (febrero 2011), Revista Investigación Desarrollo Pesquero, 23, 7–22, 2013.

Negri, R. M., Molinari, G., Carignan, M., Ortega, L., Ruiz, M. G., Cozzolino, E., Cucchi-Colleoni, A. D., Lutz, V. A., Costagliola, M., Garcia, A. B., Izzo, S., Jurquiza, V., Salomone, A., Odizzio, M., La Torre, S., Sanabria, A., Hozbor, M. C., Peressutti, S. R., Méndez, S. M., Silva, R., Martínez, A., Cepeda, G. D., Viñas, M. D., Diaz, M. V., Pajaro, M., Mattera, M. B., Montoya, N. G., Berghoff, C., and Leonarduzzi, E.: Ambiente y plancton en la zona Común de pesca argentino-uruguaya en un escenario de cambio climático (marzo, 2014), Publicaciones de la Comisión Técnica Mixta del Frente Marítimo, 251–316, 2016.

Orselli, I. B. M., Kerr, R., Ito, R. G., Tavano, V. M., Mendes, C. R. B., and Garcia, C. A. E.: How fast is the Patagonian shelf-break acidifying?, J~~ournal of~~ Mar~~ine~~ Syst~~ems~~, 178, 1–14, https://doi.org/10.1016/j.jmarsys.2017.10.007, 2018.

Osburn, C. L., Kinsey, J. D., Bianchi, T. S., and Shields, M. R.: Formation of planktonic chromophoric dissolved organic matter in the ocean, Mar Chem, 209, 1–13, https://doi.org/10.1016/j.marchem.2018.11.010, 2019.

Pasulka, A. L., Samo, T. J., and Landry, M. R.: Grazer and viral impacts on microbial growth and mortality in the southern California Current Ecosystem, J Plankton Res, 37, 320–336, https://doi.org/10.1093/plankt/fbv011, 2015.

Péquin, B., LaBrie, R., St-Gelais, N. F., and Maranger, R.: Succession of protistan functional traits is influenced by bloom timing, Front Mar Sci, 9, https://doi.org/10.3389/fmars.2022.916093, 2022.

Porter, K. G. and Feig, Y. S.: The use of DAPI for identifying and counting aquatic microflora1, Limnol Oceanogr, 25, 943–948, https://doi.org/10.4319/lo.1980.25.5.0943, 1980.

Proctor, L. and Fuhrman, J.: Roles of viral infection in organic particle flux, Mar Ecol Prog Ser, 69, 133–142, https://doi.org/10.3354/meps069133, 1991.

Redfield, A. C., Ketchum, B. H., and Richards, F. A.: The influence of organisms on the composition of sea-water, in: The sea: ideas and observations on progress in the study of the seas, vol. 2, edited by: Hill, M. N., Wiley Interscience, New York, 26–77, 1963.

Romera Romera-Castillo, C., Sarmento, H., Álvarez-Salgado, X. A., Gasol, J. M., and Marraséa, C.: Production of chromophoric dissolved organic matter by marine phytoplankton, Limnol Oceanogr, 55, 446–454, https://doi.org/10.4319/lo.2010.55.1.0446, 2010.

Romera-Castillo, C., Sarmento, H., Álvarez-Salgado, X. A., Gasol, J. M., and Marrasé, C.: Net Production production and Consumption consumption of Fluorescent fluorescent Colored colored Dissolved dissolved Organic organic Matter matter by Natural natural Bacterial bacterial Assemblages assemblages Growing growing on Marine marine Phytoplankton phytoplankton Exudatesexudates, Appl Environ Microbiol, 77, 7490–7498, https://doi.org/10.1128/AEM.00200-11, 2011.

Romero, S. I., Piola, A. R., Charo, M., and Garcia, C. a. E.: Chlorophyll- a variability off Patagonia based on SeaWiFS data, J Geophys Res, 111, 1–11, https://doi.org/10.1029/2005JC003244, 2006.

Sanders, R., Caron, D., and Berninger U, G.: Relationships between bacteria and heterotrophic nanoplankton in marine and fresh waters: an inter-ecosystem comparison, Mar Ecol Prog Ser, 86, 1–14, https://doi.org/10.3354/meps086001, 1992.

Saraceno, M., Bodnariuk, N., Ruiz-Etcheverry, L. A., Berta, M., Simionato, C. G., Beron-Vera, F. J., and Olascoaga, M. J.: Lagrangian characterization of the southwestern Atlantic from a dense surface drifter deployment, Deep Sea Research Part I: Oceanographic Research Papers Pap, 208, 104319, https://doi.org/10.1016/j.dsr.2024.104319, 2024.

Sarmento, H., Morana, C., and Gasol, J. M.: Bacterioplankton niche partitioning in the use of phytoplankton-derived dissolved organic carbon: quantity is more important than quality, ISME J, 10, 2582–2592, https://doi.org/10.1038/ismej.2016.66, 2016.

Schloss, I., Ferreyra, G., Ferrario, M., Almandoz, G., Codina, R., Bianchi, A., Balestrini, C., Ochoa, H., Ruiz Pino, D., and Poisson, A.: Role of plankton communities in sea-air variations in pCO2 in the SW Atlantic Ocean, Mar Ecol Prog Ser, 332, 93–106, https://doi.org/10.3354/meps332093, 2007.

Sherr, E. B. and Sherr, B. F.: Phagotrophic Protists: Central Roles in Microbial Food Webs, in: Aquatic Microbial Ecology and Biogeochemistry: A Dual Perspective, Springer International Publishing, Cham, 3–12, https://doi.org/10.1007/978-3-319-30259-1_1, 2016.

Sherr, E. B. and Sherr, B. F.: Heterotrophic dinoflagellates: a significant component of microzooplankton biomass and major grazers of diatoms in the sea. Mar Ecol Prog Ser, 352, 187-197, https://doi:10.3354/meps07161, 2007.

Sieburth, J. McN., Smetacek, V., and Lenz, J.: Pelagic ecosystem structure: Heterotrophic compartments of the plankton and their relationship to plankton size fractions~~–1~~, Limnol Oceanogr, 23, 1256–1263, https://doi.org/10.4319/lo.1978.23.6.1256, 1978.

Silva, R., Negri, R., and Lutz, V.: Summer succession of ultraphytoplankton at the EPEA coastal station (Northern Argentina), J Plankton Res, 31, 447–458, https://doi.org/10.1093/plankt/fbn128, 2009.

Simon, M. and Azam, F.: Protein content and protein synthesis rates of planktonic marine bacteria, Mar Ecol Prog Ser, 51, 201–213, https://doi.org/10.3354/meps051201, 1989.

Skoog, A., Thomas, D., Lara, R., and Richter, K.-U.: Methodological investigations on DOC determinations by the HTCO method, Mar Chem, 56, 39–44, https://doi.org/10.1016/S0304-4203(96)00084-9, 1997.

~~Snyder, R. A., Moss, J. A., Santoferrara, L., Head, M., and Jeffrey, W. H.: Ciliate microzooplankton from the Northeastern Gulf of Mexico, ICES Journal of Marine Science, 78, 3356–3371, https://doi.org/10.1093/icesjms/fsab002, 2021.~~

Spencer, R. G. M., Pellerin, B. A., Bergamaschi, B. A., Downing, B. D., Kraus, T. E. C., Smart, D. R., Dahlgren, R. A., and Hernes, P. J.: Diurnal variability in riverine dissolved organic matter composition determined by *in situ* optical measurement in the San Joaquin River (California, USA), Hydrol Process, 21, 3181–3189, https://doi.org/10.1002/hyp.6887, 2007.

Staniewski, M. A. and Short, S. M.: Potential viral stimulation of primary production observed during experimental determinations of phytoplankton mortality. Aquat Microb Ecol, 71, 239-256, https://doi.org/10.3354/ame01679, 2014.

Stedmon, C. A. and Bro, R.: Characterizing dissolved organic matter fluorescence with parallel factor analysis: a tutorial, Limnol Oceanogr Methods, 6, 572–579, https://doi.org/10.4319/lom.2008.6.572, 2008.

Stedmon, C. A., Markager, S., and Bro, R.: Tracing dissolved organic matter in aquatic environments using a new approach to fluorescence spectroscopy. Mar Chem, 82(3-4), 239-254, https://doi.org/10.1016/S0304-4203(03)00072-0, 2003.

Suttle, C. A.: Viruses in the sea, Nature, 437, 356–361, https://doi.org/10.1038/nature04160, 2005.

Taylor, A. and Landry, M.: Phytoplankton biomass and size structure across trophic gradients in the southern California Current and adjacent ocean ecosystems, Mar Ecol Prog Ser, 592, 1–17, https://doi.org/10.3354/meps12526, 2018~~a~~.

~~Taylor, A. and Landry, M.: Phytoplankton biomass and size structure across trophic gradients in the southern California Current and adjacent ocean ecosystems, Mar Ecol Prog Ser, 592, 1–17, https://doi.org/10.3354/meps12526, 2018b.~~

Taylor, G. T., Iturriaga, R., and Sullivan, C. W.: Interactions of bactivorous grazers and heterotrophic bacteria with dissolved organic matter, Mar~~.~~ Ecol~~.~~ Prog~~.~~ Ser, 60, 1884–1888, https://doi.org/10.3354/meps023129, 1985.

Timko, S. A., Maydanov, A., Pittelli, S. L., Conte, M. H., Cooper, W. J., Koch, B. P., Schmitt-Kopplin, P., and Gonsior, M.: Depth-dependent photodegradation of marine dissolved organic matter, Front Mar Sci, 2, https://doi.org/10.3389/fmars.2015.00066, 2015.

Tremaine, S. C. and Mills, A. L.: Tests of the cCritical aAssumptions of the dDilution mMethod for eEstimating bBacterivory by mMicroeucaryotes, Appl Environ Microbiol, 53, 2914–2921, https://doi.org/10.1128/aem.53.12.2914-2921.1987, 1987.

Urban-Rich, J., McCarty, J. T., and Shailer, M.: Effects of food concentration and diet on chromophoric dissolved organic matter accumulation and fluorescent composition during grazing experiments with the copepod Calanus finmarchicus, ICES Journal of Marine Science, 61, 542–551, https://doi.org/10.1016/j.icesjms.2004.03.024, 2004.

Ward, B. A. and Follows, M. J.: Marine mixotrophy increases trophic transfer efficiency, mean organism size, and vertical carbon flux, Proceedings of the National Academy of Sciences, 113, 2958–2963, https://doi.org/10.1073/pnas.1517118113, 2016.

Weinbauer, M. G. and Peduzzi, P.: Significance of viruses versus heterotrophic nanoflagellates for controlling bacterial abundance in the northern Adriatic Sea, J Plankton Res, 17, 1851–1856, https://doi.org/10.1093/plankt/17.9.1851, 1995.

Weisse, T., Anderson, R., Arndt, H., Calbet, A., Hansen, P. J., and Montagnes, D. J. S.: Functional ecology of aquatic phagotrophic protists — Concepts, limitations, and perspectives, Eur J Protistol, 55, 50–74, https://doi.org/10.1016/j.ejop.2016.03.003, 2016.

Zhao, Z., Li, H., Sun, Y., Shao, K., Wang, X., Ma, X., Hu, A., Zhang, H., and Fan, J.: How habitat heterogeneity shapes bacterial and protistan communities in temperate coastal areas near estuaries, Environ Microbiol, 24, 1775–1789, https://doi.org/10.1111/1462-2920.15892, 2022.

Zheng, Q., Chen, Q., Cai, R., He, C., Guo, W., Wang, Y., Shi, Q., Chen, C., and Jiao, N.: Molecular characteristics of microbially mediated transformations of Synechococcus-derived dissolved organic matter as revealed by incubation experiments, Environ Microbiol, 21, 2533–2543, https://doi.org/10.1111/1462-2920.14646, 2019.